Comparative Biochemistry and Physiology, Part B 258 (2022) 110698

Contents lists available at ScienceDirect

Comparative Biochemistry and Physiology, Part B

journal homepage: www.elsevier.com/locate/cbpb

Research Article

Molecular and functional characterization of a SCD 1b from European sea bass (*Dicentrarchus labrax* L.)

Almudena González-Rovira [a], Gabriel Mourente [b], José Manuel Igartuburu [c], Carlos Pendon [a,*]

[a] Departamento de Biomedicina, Biotecnología y Salud Pública, INBIO, Facultad de Ciencias, Universidad de Cádiz, 11519 Puerto Real, Cádiz, Spain
[b] Departamento de Biología, Facultad de Ciencias del Mar y Ambientales, Universidad de Cádiz, 11519 Puerto Real, Cádiz, Spain
[c] Departamento de Química Orgánica, INBIO, Facultad de Ciencias, Universidad de Cádiz, 11519 Puerto Real, Cádiz, Spain

ARTICLE INFO

Edited by Chris Moyes

Keywords:
SCD 1b
Δ6 FAD
Molecular cloning
Functional characterization
MUFAs
Dicentrarchus labrax L.
3D protein structure
Substrate specificity
Substrate preference

ABSTRACT

Fatty acid desaturation is a highly complex and regulated process involving different molecular and genetic actors. Ultimally, the fatty acid desaturase enzymes are responsible for the introduction of double bonds at different positions of specific substrates, resulting in a wide variety of mono- and poly-unsaturated fatty acids. This substrate-specificity makes it possible to meet all the functional needs of the different tissues against a wide variety of internal and external conditions, giving rise to a varied profile of expression and functionality of the different desaturases in the body. Being our main interest to study and characterize at the molecular level the fatty acid desaturation process in fishes, we have focused our effort on characterizing SCD 1b from European sea bass (*Dicentrarchus labrax*, L.). In this work, we have characterized a tearoyl-CoA Desaturase cDNA that codes a protein of 334 amino acids, which shares the greatest homology to marine fish SCD 1b. Northern blot analysis showed two transcripts of 3.5 kb and 1.4 kb. Two putative *cis*-acting conserved motifs are localized in the cDNA 5′-end: a polypyrimidine CT dinucleotide repeat tract and two non-palindromic putative NRL-response elements (NREs). The deduced protein presents two Δ9 FADs like domain, three His-rich motifs, a total of nine His residues acting as di-iron coordination ligands. The SCD 1b 3D protein modelling shows a structure made up primarily of α-helices, four of which could be transmembrane helices. The catalytic region is oriented to the cytosolic side of the Endoplasmic Reticulum membrane, where the 9-histidine residues are arranged coordinated to two non-heme Fe^{2+} ions. A new His-containing motif NX_3H-like includes an Asn residue that participates in the coordination of $Fe^{2+}1$ through a water molecule. The protein has a large pocket with a large opening to the outside. It includes a tunnel in which the substrate-binding site is located. The external shape is reminiscent of a boathook. It shows group specificity, although a greater preference for 18C substrates. The length of the tunnel, delimited by seven amino acids that forms a pocket at the end of the tunnel, the possibility that the substrates adopt different conformations inside the tunnel as well as and the movement of acyl chain inside the tunnel, could explain the high preference for 18C fatty acids and the group specificity of the enzyme. The cDNA encodes a functional SCD enzyme, whose subcellular localization is the Endoplasmic Reticulum, which complements the *ole1*Δ gene-disrupted gene in DTY-11A *Saccharomyces cerevisiae* strain and produces an increment of palmitoleic and oleic acids. The *scd 1b* gene is expressed in all tested tissues, showing the liver and adipose tissue a higher level of expression against the brain, heart, gonad and intestine. *Scd 1b* expression was always bigger than those of the *Δ6 fad* gene, being especially significant in adipose tissue and liver. From our data, we conclude that, in contrast to the functional significance of SCD 1b in adipose tissue, liver and heart, Δ6 FAD seems to play a more determining role in the biosynthesis of unsaturated fatty acids in the intestine, brain and gonad in fish.

Abbreviations: AREs, AU-rich elements; ER, Endoplasmic reticulum; FA, Fatty Acid; FAD, Fatty Acid Desaturase; FAME, Fatty Acid Metil-Ester; *GAPDH*, Glyceraldehyde-3-phosphate dehydrogenase gene; MUFA, Monounsaturated Fatty Acid; NRE, NRL-response element; NRL, Neural Retinal Leucine Zipper; pI, Isoelectric point; ORF, Open Reading Frame; RACE, Rapid Amplification of Complementary DNA Ends; RT-qPCR, Real-Time quantitative PCR; RTR, Relative Transcription Ratio; SCD, Stearoyl-CoA Desaturase or Δ9-FAD; *scd 1b*, Stearoyl-CoA 1b Desaturase gene or mRNA; SFA, Saturated Fatty Acid; UFA, Unsaturated Fatty Acid; UTR, Untranslated Region; Δ6 FAD, Δ6-Fatty Acid Desaturase; *Δ6 fad*, Δ6-Fatty Acid Desaturase gene or mRNA.

* Corresponding author.
E-mail addresses: almudena.gonzalez@uca.es (A. González-Rovira), gabriel.mourente@uca.es (G. Mourente), josemanuel.igartuburu@uca.es (J.M. Igartuburu), carlos.pendon@uca.es (C. Pendon).

https://doi.org/10.1016/j.cbpb.2021.110698
Received 11 August 2021; Received in revised form 11 November 2021; Accepted 12 November 2021
Available online 19 November 2021

Editor: Chris Moyes

1. Introduction

Fatty acid desaturation is a highly complex and regulated process involving different molecular and genetic actors. Ultimately, the fatty acid desaturase (FAD) enzymes are responsible for the introduction of double bonds at different positions of specific substrates, resulting in a wide variety of mono- and poly-unsaturated fatty acids. This substrate-specificity makes it possible to meet all the functional needs of the different tissues against a wide variety of internal and external conditions, giving rise to a varied profile of expression and functionality of the different desaturases in the body. In animals, not only does the SCD play a relevant role in this process, but also other desaturases can play a relevant role in response to the environmental conditions and the functional needs of the different tissues. Thus, in marine fish, the specific function of Δ6 FAD is still unclear and the specific role that both enzymes play is not well established. Stearoyl-CoA desaturase (SCD) (EC 1.14.19.1) is an Acyl-CoA desaturase associated to Endoplasmic Reticulum membrane. This enzyme introduces the first *cis*-double bond at the 9, 10 position in saturated fatty acids (SFAs), primarily 16:0 and 18:0, to produce monounsaturated fatty acids (MUFAs), such as 16:1n-7 and 18:1n-9, respectively (Flowers and Ntambi, 2008). SCD enzyme, together with NADH cytochrome *b*5 reductase and cytochrome *b*5, forms a multienzyme system. In the unsaturation process, the membrane-bound cytochrome *b*5 transfers electrons by lateral diffusion from NADH cytochrome *b*5 reductase to the SCD (Heinemann and Ozols, 2003). An *N*-terminal Cytochrome b5-like domain is present in other FADs (Δ5 and Δ6 FADs) but not in SCD (Guillou et al., 2004). However, in yeast (*Saccharomyces cerevisiae*) SCD (OLE1) a *C*-terminal cytochrome *b*5-like motif is present, which is essential for its activity (Mitchell and Martin, 1995). These enzymes present three histidine-rich motifs containing residue essential for its catalytic activity since they bind the iron atoms within the catalytic center (Shanklin et al., 1994). From the structural point of view, the crystal structure of mouse SCD 1 has recently been resolved. The folding of the polypeptide chain comprises four transmembrane helices that support a cytosolic domain in which the active center of the enzyme is located (Bai et al., 2015). SCD is the key enzyme in MUFA biosynthesis, which are key substrates for the formation of most acyl lipids, membrane phospholipids, cholesterol esters and triglycerides. The molecular species of phospholipid classes, denoted by their specific fatty acyl composition, play crucial roles in the maintenance of membrane features necessary for a correct cellular function. Thus, the unsaturation level of fatty acid (FA) in cell membranes is considered as an important mechanism of temperature stress adaptation in living organisms, including fish (Cossins and Bowler, 1987; Wodtke and Cossins, 1991). In addition, the alteration of phospholipid acyl composition in membranes is closely related to the molecular basis of a great variety of potential diseases including cancers, diabetes and cardiovascular disorders (reviewed in Mauvoisin and Mounier, 2011).

The number of SCD isoforms is broadly variable among species. In mammals, four isoforms of SCD (SCD-1 to −4) have been identified in mouse (*Mus musculus*) (Nakamura and Nara, 2004), two (SCD-1 and -2) in rat (*Rattus norvegicus*) (Mihara, 1990) and two (SCD-1 and -5) in humans, not having been found so far in teleost fish the SCD-5 isoform (Castro et al., 2011; Wang et al., 2005; Wu et al., 2013; Zhang et al., 1999). In fish, two variant of the SCD 1 gene has been reported in common carp (*Cyprinus carpio*) (Tiku et al., 1996), red sea bream (*Pagrus major*) (Oku and Umino, 2008) and gilthead sea bream (*Sparus aurata*) (Benedito-Palos et al., 2013). Nevertheless only one variant in species such as grass carp (*Ctenopharyngodon idella*) (Chang et al., 2001), milkfish (*Chanos chanos*) (Hsieh et al., 2001) and tilapia (*Oreochromis mossambicus*) (Hsieh et al., 2004). SCD cDNAs have been cloned in some fish species: zebrafish (*Danio rerio*), Fugu (*Takifugu rubripes*), tilapia (*O. mossambicus*), grass carp (*C. idella*), common carp (*C. carpio*), the Antarctic species *Chionodraco hamatus* and *Trematomus bernacchii*, gilthead sea bream *(S. aurata*) and milkfish (*C. chanos*). However, only SCD cDNA from *Mortierella alpine* (Abe et al., 2006), domestic fly (*Musca domestica*) (Eigenheer et al., 2002), the marine copepod *Calanus hyperboreus* (Meesapyodsuk and Qiu, 2014) and the cephalopod common octopus (*Octopus vulgaris*) (Monroig et al., 2017) has been functionally characterized. To our knowledge, not any SCD cDNA from a teleost fish has been functionally characterized. At a structural level, the crystal structure of human and mouse SCD 1 containing two Zn^{2+} ions instead of two Fe^{2+} ions has recently been resolved at 2.6 Å and 3.3 Å respectively (Bai et al., 2015; Wang et al., 2015), but both proteins turned out not to be functional. Furthermore, the crystal structure of mouse SCD 1 containing two ferrous ions has been resolved at 3.5 Å, resulting in a fully functional protein (Shen et al., 2020).

The European sea bass (*D. labrax*) is one of the most important carnivorous marine finfish species cultured in European waters, showing high commercial interest. Thus, the total aquaculture production of Sea bass in Europe and the rest of the Mediterranean Arc in 2019 was 212,977 tons, being the total value at the first sale of 1064.9 million euros (APROMAR, 2020).

Being our main interest is to study and characterize at the molecular level the fatty acid desaturation process in fish, we have focused our effort on characterizing SCD 1b from European sea bass (*D. labrax*, L.). Thus, our work has been to molecular and functionally characterizing this key enzyme in the metabolism of unsaturated fatty acids of teleost fishes, as well as deepening its 3D structure through the in silico homology modelling study. In a previous work (González-Rovira et al., 2009) we have cloned and characterized a component of the FA desaturation system in this species, which resulted to be a gene for the Δ6 FAD enzyme. Moreover, in the present work it is described the molecular and functional characterization of the main gene product from *D. labrax* that shows Δ9-fatty acyl desaturase activity and can repair the monounsaturated FA auxotrophy when it is expressed in DTY-11A *S. cerevisiae* strain, which is defective in SCD activity. Therefore, we have analyzed its transcription in different tissues (brain, heart, gonad, liver, intestine and adipose tissue). We have determined the subcellular localization of the protein products encoded in the cDNA and we have modelled the deduced polypeptide chain, to propose a functional structure of this enzyme, which we have used to explain and justify its group specificity and its greater preference for 18C substrates. By last, we have studied the functional relationship between two enzymes with desaturase activity of this complex system: a new SCD 1b, the broadly SCD expressed in fish, and a Δ6 FAD, from a marine vertebrate, the European sea bass.

2. Materials and methods

2.1. Fish

European sea bass (*D. labrax* L.) weighing 800–900 g were supplied by the "Laboratorio de Cultivos Marinos", University of Cádiz, Puerto Real, Spain. Fish were grown in a well seawater flow through system, at a constant temperature and salinity of 19 ± 1 °C and 39 ppt, respectively, and natural photoperiod conditions. Fish were fed by automatic feeders with commercial 2 mm dry pellets (Skretting España S.A, Burgos, Spain) to apparent satiation (daily ration about 1% body weight). Fishes were fasted for 24 h before sampling. Animals were anaesthetized in MS-222 (Sigma, St Louis, MO; 100–200 mg/L of water) before sacrifice. All the procedure was conducted according to the European Union directive (2010/63/EU) for the protection of animals used for experimental and other scientific purposes.

2.2. RNA isolation and molecular cloning

Total RNA was obtained from European sea bass brain tissue using TRIsure™ Reagent (Bioline, London, UK) following the manufacturer's instructions. Genomic DNA was eliminated by DNase I treatment (USB,

UK). Five μg of total RNA were reverse-transcribed into cDNA using SuperScript III RT reverse transcriptase (Invitrogen, Carlsbad, USA), primed by the oligonucleotide *Not* I-oligo-dT, which include a *Not I* restriction site (underline) (Table 1). Reverse transcription products were RNase H treated (Invitrogen, Carlsbad, USA) and cDNA was purified by filtration using a Centri-sep column (Princeton Separation, Adelphia, NJ). A homopolymeric dC tail was added to the 3′ end of cDNA using Terminal Deoxynucleotidyl Transferase (Invitrogen, Carlsbad, USA) and the tailed cDNA was directly used for PCR amplification assays.

A cDNA, including a complete ORF for a putative SCD, was obtained by PCR. Firstly, 3′- RACE was used to obtain an SCD European sea bass cDNA fragment. Primers were designed from a consensus analysis of conserved coding regions of known fish stearoyl-CoA sequences available in the GenBank database (http://www.ncbi.nlm.nih.gov). A degenerate forward primer, with the sequence codon usage optimized for European sea bass, and the reverse primer *Not* I-oligo-dT (Table 1), were used to obtain the first fragment of 837 bp of SCD European sea bass. PCR was performed in a final volume of 50 μL, using high-fidelity Kod Hot Start Polymerase (Novagen, Darmstadt, Germany), under the following conditions: initial denaturation at 94 °C for 2 min, 45 cycles of 94 °C for 15 s, 57 °C for 30s, 72 °C for 2 min and a final extension step of 72 °C for 7 min. The PCR products were gel purified and cloned into TOPO-TA cloning vector (Invitrogen, Carlsbad, USA) following the manufacturer's instructions. The consensus sequence obtained from five positive clones was further employed for specific primers design in the following Rapid Amplification of cDNA End (RACE) experiment. 5′ RACE was carried out using a specific reverse primer together with a forward Not I-oligo-dG primer (Table 1). A touchdown PCR was performed, where the annealing temperature was set between 68 °C and 57 °C for 30s for 45 cycles, using Eco Taq DNA polymerase (Ecogen, Madrid, Spain). Following the above strategy, an overlapping fragment of 702 bp was acquired and a contig nucleotide sequence was obtained. Finally, two specific primers were designed (Table 1) to PCR amplify the full cDNA of the putative Sea bass SCD. Amplification conditions were: an initial step at 94 °C for 2 min followed by 45 cycles of 94 °C for 30 s, 56 °C for 30 s, 72 °C for 1 min and a final extension step of 72 °C for 7 min, using a high-fidelity Kod Hot Start Polymerase (Novagen, Darmstadt, Germany), in a final volume of 50 μL. PCR products were gel purified, cloned and sequenced as it is previously described. Nine clones containing the appropriate product were sequenced to unequivocally confirm the complete sequence of the sea bass SCD mRNA (GeneBank accession no. **FN868643**).

Table 1
Used primers.

Primer (5′-3′)	Used for
ATGCACCCCYTCTTCTTCGCC (F)[a]	First fragment of sea bass SCD cDNA cloning
ATAAGAATGCGGCCGC$(T)_{20}$ V (R)[b]	
ATAAGAATGCGGCCGCTAAA$(G)_{15}$H (F)[b]	Second fragment of sea bass SCD cDNA cloning
GTCGGCACAAGGAAGCAAAGGAT (R)[b]	
ACTCTCTGTCTCTCTCTGTCTC (F)[b]	Full-length of sea bass SCDcDNA cloning
ATATTATGGTGAAAAAGCTGTG (R)[b]	
TGTTACGGATCCACTTCAGCAAAA (F)[b]	Functional characterization of sea bass ORF cDNA (Bam HI site and Eco RI site are underlined)
TATGAATTCGCGGAGTTTGTAGC (R)[b]	
GCTTCCACAACTACCATCACAC (F)[b]	*Sea bass SCD 1b* RT-qPCR
GGACTCAACCACTTTTGTAGCC (R)[b]	
CAAGATCATTGCCCCACCTGAG (F)[b]	*β-ACTIN* RT-qPCR
GCAGATGTGGATCAGCAAGCAG (R)[b]	
GTGCCAGCCAGAACATCATCC (F)[b]	*GAPDH* RT-qPCR
GGACAGTCAGGTCAACCAC (R)[b]	
AACGAATTCAGCAAAATGACCGAAACG (F)[b]	Subcellular localization (Eco RI and Bam HI sites are underlined)
ATGGATCCCACTTTTGTAGCCTCCGTCAC (R)[b]	

The symbols used to donate multiple nucleotides are: V = A, G or C and H = A, C or T. (F): Forward. (R): Reverse.
[a] Degenerate primer.
[b] SCD 1b specific primer.

2.3. Northern blot analysis

Northern blot analysis was carried out as previously describe Pendón et al. (1994). Thirty μg of total RNA were subjected to electrophoresis on a 1.2% agarose-2.2 M formaldehyde denaturing gel and then transferred onto nylon filters (Pall Corporation, Florida, USA). The obtained SCD cDNA was ^{32}P labelled by random priming and used as a specific probe to hybridize the membrane at 60 °C, during 16 h in 5 x SSC (750 mM NaCl, 75 mM sodium citrate). For Δ6 FAD and β-actin Northern analysis, ^{32}P labelled cDNAs previously cloned were used as specific probes (35). The membranes were washed twice under high-stringency conditions (0.1 x SSC, 0.5% SDS) for 30 min at 65 °C and then were autoradiographed for six hours (β-actin), one night (SCD) or three days (Δ6 FAD), with Curix RP2 film (Agfa, Barcelona, Spain) with an intensifying screen at −80 °C. RNA from three individuals was assayed in three different membranes using the same hybridization and washed conditions to confirm the results.

2.4. DNA and protein in silico sequence analysis

The cDNA and deduced amino acid sequences were used as a query in the public database using BLAST tools searches (http://blast.ncbi.nlm.nih.gov). Multiple sequence alignments of stearoyl-CoA desaturase were performed with the CLUSTAL omega algorithm (http://www.ebi.ac.uk/Tools/msa/clustalo/). The evolutionary history was inferred using the Neighbor-Joining method (Saitou and Nei, 1987). The evolutionary distances were computed using the p-distance method (Nei and Kumar, 2000). Evolutionary analyses were conducted in MEGA6 software (Tamura et al., 2013). Conserved domains were investigated using the Conserved Domain Search tool at NCBI (http://www.ncbi.nlm.nih.gov/Structure/edd/wrpsb.cgi). Secondary structure and transmembrane expanded helix predictions were investigated using ANTHEPRO 2000 v.60 software, included in the software packages tool for secondary structure at ExPASy Proteomics Server (http://www.expasy.ch/), SVMtm Transmembrane Domain Predictor bioinformatic tool (Yuan et al., 2004) in the ARC Center of Excellence in Bioinformatics (http://bioinformatics.org.au/), Predictprotein software (http://www.predictprotein.org), HMMTOP version 2.0 software (Tusnády and Simon, 1998, 2001) and TOPCONS membrane topology prediction software (Bernsel et al., 2009) (http://topcons.cbr.su.se/). For protein modelling, 3D structure prediction and analysis of polypeptide chain, SWISS-MODEL server (https://swissmodel.expasy.org/) and the Phyre2 web portal (http://www.sbg.bio.ic.ac.uk/phyre2/) (Kelley et al., 2015) were used. The generated models were further verified by using the structures assessment tool in the SWISS-MODEL server. Energy minimization was performed using the YASARA Energy Minimization Server (Krieger et al., 2009). The active site of the enzyme was investigated and analyzed using CASTp server (http://sts.bioe.uic.edu/castp/calculation.html/) (Tian et al., 2018). The docking of the different substrates and the enzyme was studied using the software Autodock Tools ver. 1.5.7 (https://ccsb.scripps.edu/mgltools/). 3D structure and interatomic distances were estimated by the UCSF Chimera software ver. 1.15 (https://www.rbvi.ucsf.edu/chimera) (Pettersen et al., 2004).

2.5. Functional characterization of sea bass SCD cDNA

Functional characterization of the putative open reading frame (ORF) was performed by its heterologous expression in the yeast *S. cerevisiae*, to determine the specific enzymatic activity of the putative SCD protein. Specific primers containing appropriate restriction sequences (Table 1) were designed for PCR cloning of the European sea bass putative SCD cDNA ORF into the pYES2 expression vector (Invitrogen, Carlsbad, USA), using a high-fidelity DNA polymerase (KOD

HOT Start DNA Polymerase, Novagen, Germany). The amplification involved an initial denaturation step at 94 °C for 2 min, followed by 30 cycles of denaturation at 94 °C for 30s, annealing at 62 °C for 30s and extension at 72 °C for 1 min. The PCR product was gel purified, restriction endonucleases digested and ligated into the pYES2 yeast expression vector restricted with the same enzymes. Thus the ORF was under the control of the inducible *GAL-1* promoter. Ligation was transformed into Top10 *Escherichia coli* chemically competent cells (Invitrogen, Carlsbad, USA). After sequence confirmation, recombinant plasmid pD9D/pYES2 was transformed into *S. cerevisiae* strain INVSc1 (Invitrogen, Carlsbad, USA) using S.c. EasyComp Transformation kit (Invitrogen, Carlsbad, USA), following the manufacturer's instructions. Selection of yeasts containing pD9D/pYES2 plasmid was carried out on *S. cerevisiae* minimal medium minus uracil (SCMM$^{-uracil}$). Induction of putative SCD was carried out in SCMM$^{-uracil}$ broth, using galactose (2.0% final concentration) for gene expression, as described previously González-Rovira et al. (2009). Yeast transformed with empty pYES2 plasmid (E/pYES2) was used as control. All assays were in duplicate. After 18 and 48 h of induction at 28 °C yeast were harvested, washed, dried and lipid extracted by homogenization in chloroform/methanol (2:1 by vol.) containing 0.01% butylated hydroxytoluene (BHT) as an antioxidant, according to the Folch method (Folch et al., 1957). FAMEs were prepared and analyzed according to Yadav et al. (2007), using a Varian Saturn 2200 GC–MS equipped with a supelcowax 10 M capillary column (30 m × 0.25 mm). Generated data were used to calculate the conversion of FA substrates (18:0 and 16:0) to desaturated products (18:1 and 16:1). Conversions were calculated from the gas chromatograms, as percentage of product area per total of product and substrate areas (100 × [product area / (product area + substrate area)]). Unequivocal confirmation of FA products was obtained by GC–mass spectrometry of the picolinyl derivatives as previously described in detail Hastings et al. (2001).

2.6. Yeast complementation

In a second assay, the recombinant plasmids pD9D/pYES2 was transformed into *ole1 HpaIΔ::LEU2*, DTY-11A yeast, an *S. cerevisiae* strain (MAT α, *ole1Δ*::*LEU2*, *leu2–3*, *leu2–112*, *his3–11*, *his3–15*, *trp1–1*, *can1–100*, *ura3–1*, *ade2–1*(HIS^{+})) which contains gene-disrupted forms of *OLE1*. This strain is defective in SCD activity and MUFAs synthesis and requires palmitoleic and oleic FAs in the medium for growth (0.5 mM each final concentration). Selection of yeasts containing pD9D/pYES2 was carried out on *S. cerevisiae* minimal medium minus leucine (SCMM$^{-leucine}$). To induce transcription of the putative Δ9 FAD enzyme, galactose (2.0% final concentration) was added to the medium without palmitoleic (16:1 n-7) and oleic (18:1 n-9) FAs. After 96 h of induction, FA profile analysis was performed as described above. An *ole1 HpaIΔ::LEU2*, DTY-11A strain transformed with E/pYES2 plasmid grown in SCMM$^{-leucine}$ medium containing palmitoleic (0.5 mM) and oleic (0.5 mM) FAs, was used as control. All assays were in duplicate. Conversion of FA substrates (18:0 and 16:0) to desaturated products (18:1 and 16:1 respectably) was calculated as is described previously.

2.7. Subcellular localization of the protein product of the SCD ORF cDNA

Subcellular localization of the putative SCD encoded in the ORF cDNA was carried out, as previously describe González-Rovira et al. (2009), in DLEC, an embryonic cell line from sea bass (Buonocore et al., 2006). The ORF of sea bass SCD 1b was obtained by PCR amplification using D9LuGFPF and D9LuGFPR primers (Table 1). Amplification was carried out in a final volume of 50 μL, using full length cDNA previously obtained as template and a high fidelity hot start polymerase (KOD HOT Start, Novagen, Cerdanyola, Spain). PCR conditions were initial step at 94 °C for 2 min, 25 cycles of denaturation at 94 °C for 30 s, annealing at 62 °C for 30 s and 72 °C for 2 min and a final extension step of 72 °C for 7 min. The PCR fragment was gel purified, *Eco* RI and Bam HI restricted and ligated into gel-purified mammalian expression vector pEGFP-N1 (Clontech, Madrid) previously digested with the same restriction enzymes. Ligation was transformed in Top-10 *E. coli* chemically competent cells (Invitrogen, Barcelona, Spain). The plasmid pSCD1b-EGFP was sequenced to confirm the nucleotide sequence. One μg of each pSCD1b-EGFP and pDsRed2-ER (Clontech, Madrid, Spain) plasmid were co-electroporated into DLEC cell to confirm the location of SCD 1b in the endoplasmic reticulum. Electroporation conditions were as follow: 1E5 cell/100 μL were transfected using one pulse of 15 milliseconds, 160 V and a square pulse type in a Gene Pulser Xcell (BioRad, USA). After 48–72 h, cells were observed in a Motic AE31 inverted microscopy (Motic, China) for the presence of green fluorescent fusion protein (SCD1b-EGFP) and red fluorescence of DsRed2-ER. Images were taken using a 50× immersion oil objective and a MotiCam 5000 cool digital camera (Motic). Quantitative co-localization was performed using ImageJ 1.53e Software (https://imagej.nih.gov/). Pearson's correlation coefficient (r_p), Overlap coefficient (r) (Manders et al., 1992) and Li's Intensity Correlation Quotient (ICQ) (Li et al., 2004) were used to evaluate the co-localization of green and red fluorescence in the images.

2.8. Transcriptional analysis: RNA extraction and real time quantitative-PCR (RT-qPCR)

Quantitative tissue distribution analysis of European sea bass SCD gene was performed by RT-qPCR. Six tissues (brain, heart, gonad, liver, adipose tissue and intestine) were extracted in RNAlater Storage Solution (SIGMA) and immediately stored at −80 °C. Total RNA was obtained using TRIsure™ (Bioline) following the manufacturer's protocol. One and a half μg of total RNA was reverse-transcribed into cDNA using iScript™ cDNA Synthesis kit (Bio-Rad, Alcobendas, Madrid). Primers for qPCR analysis were designed in the coding region (Table 1) to obtain a PCR product size of 198 bp. Amplifications were performed in a Mini-Opticom Real Time PCR System (Bio-Rad, USA), using the 2× Sensimix dU SYBR Green Kit (Quantace, UK), in 20 μL final volume. qPCR conditions were as follow: an initial step at 95 °C for 3 min, 35 cycles of denaturation at 95 °C for 10 s, annealing at 63 °C for 10 s and 72 °C for 10 s. Quantitative transcription analysis of Δ6 *fad* was performed as described González-Rovira et al. (2009). Data were normalized against β-actin (GenBank accession no. **AY148350**) transcription, using the ΔC_T method. All amplicons (SCD, Δ6 FAD and β-actin) were verified by sequencing.

For tissue distribution transcription analysis of Sea bass SCD mRNA, the absolute quantification method was performed using standard curves of five points of 10-fold serial dilutions of cDNA of each tissue, to assess reaction optimization and proper quantification. Samples from five individuals were tested. However, three technical replicates and cDNA from 25 ng of total RNA per replica were assayed. All amplifications were followed by a melting curve analysis to confirm that a single PCR product was amplified. To evaluate the SCD/Δ6 FAD Relative Transcription Ratio (RTR), obtained absolute and relative (ΔC_T) transcription values of both genes from each individual were used to calculate the ratio. Then the mean value for every five animals of each group was compared. All quantitative analyses were performed using CFX Analysis Software v.3.1 (Bio-Rad, Alcobendas, Madrid).

2.9. Theoretical and statistical analysis

All results are reported as means ± SEM ($n = 5$) unless otherwise stated. All statistical analyses were performed using a statistical computer package (Prism 4.0, GraphPad Software, Inc., San Diego, California, USA). The statistical significance was determined by one-way ANOVA followed, where appropriate, by Tukey's multiple comparison test. Percentage data and data which were identified as nonhomogeneous (Bartlett's test) were subjected to either arcsine, square root or log transformation before analysis. Differences were reported as significant if $p < 0.05$ (Zar, 1984).

3. Results

3.1. Cloning and sequence analyses of full-length cDNA for SCD of European sea bass

A full-length cDNA of 1,366 bp for a stearoyl-CoA desaturase from European sea bass, was obtained (GenBank accession no. **FN868643**), containing an 85 bp 5′ untranslated region (UTR), a 276 bp 3′ UTR and a 1005 bp ORF (Supplementary Fig. S1), which encode a protein of 334 amino acids (Fig. 1) with an estimated molecular weight of 37.8 kDa and a theoretical pI of 9.26. The 5′-end region of cDNA contains putative *cis*-acting conserved sequences related to the control of the gene expression. Within the 5′-UTR a polypyrimidine CT dinucleotide repeat element (nucleotide 2–40) is present. Additionally, two nonpalindromic putative NRL-response elements (NRE), with the consensus sequence (TGC(N_{3-4})GCA) (Kerppola and Curran, 1994), are present in the 5′-end of the cDNA. The first NRE is localized in the 5′-UTR (nt 48–59) and the second is localized in the coding region (nt 356–368). The 3′-UTR does not include the standard poly-A tail (AATAAA) signal, although alternatives sequences (CATAAA and two-overlapped AATATA and TATAAA) are present. In addition, AU-rich elements (AREs), related to mRNA instability, were not present in the 3′ UTR of the obtained cDNA (Supplementary Fig. S1).

Northern blots analysis from the liver of three individuals showed two putative transcripts, whose estimated sizes were 3.5 kb and 1.4 kb, respectively (Fig. 2). The largest transcript showed the highest level of transcription. However, the 1.4 kb transcript accurately matches the length of the cDNA obtained in this work.

3.2. In silico analysis of the deduced protein sequence

3.2.1. Deduced protein structure analysis

The predicted protein shows all characteristic motif and domains previously described for other SCD. Two Δ9-FADS-like domains (amino acids 75 to 162 and amino acids 223 to 312) and three histidine-rich regions (His-box), one HX_4H-like and two HX_2HH-like, are found at the same relative position as in other species (Fig. 1). These motifs together with an additional His residue (H244), also conserved (Fig. 1) may function as non-heme di-iron binding sites, being essential for SCD activity (Shanklin et al., 1994; Bai et al., 2015). As in other members of the SCD family, the deduced protein lacks a cytochrome *b*5-like motif, unlike what happens in other SCDs, such as the SCD (OLE1) from yeast (*S. cerevisiae*) (Mitchell and Martin, 1995) or in other members of the fatty acids desaturase family, as the Δ6 FAD (Guillou et al., 2004).

Amino acid sequence alignment of the predicted protein with SCD 1 from other fish species indicated a high level of conservation (Fig. 1). Sequence identity with other SCD of fish was above 68.5%, being above 75% when compared to other SCD 1b of fish. The greatest amino acid identity was shown to marine fish SCD 1: Sea bream (87.7%), Fugu 2 (81.3%), and Atlantic salmon (75.8%) (Table 2). Consistent with this result, phylogenetic analysis grouped the Sea bass SCD sequence with the same species into the SCD 1b group (Fig. 3). The identity with other fish SCD 1a descends from 74.6% (Grass carp) to 68.5% (Antarctic icefish). This SCD 1a group appears in a different branch in the phylogenetic tree. A third group of SCD sequences of Zebrafish and Milkfish presents a percentage of identity between 74.3% and 68.9%, which appears grouped in a third separated branch (Fig. 3).

Analysis for secondary structure prediction shows, with high confidence, the protein is mainly composed of α-helices and disordered structures alternating in the primary structure (Supplementary Fig. S2A). The protein would be composed of 14 α-helices (H1-H14). The hydrophobicity plot of the putative SCD 1b protein, revealed the presence of six highly hydrophobic regions (Supplementary Fig. S2C), which included four possible transmembrane segments (TMS1-TMS4) (Supplementary Fig. S2A, B), being the three histidine-rich regions (His-box), the conserved H244 and the N- and C-terminal-end on the cytosolic side of the endoplasmic reticulum membrane (Supplementary Fig. S2B). On the model, TMS2 and TMS4 are longer than TMS1 and TMS3. In TMS2, H95 and H100 residues and in TMS4, H244 residue, all involved in the coordination of metal ions, are located at its cytosolic C-terminus (Supplementary Fig. S2A, B). All transmembrane helices include polar amino acids at the ends that project into the cytosol, except TMS3. The hydrophobic profile of some α-helices indicates that they are embedded in the membrane of the endoplasmic reticulum without reaching through it (H3, H12 and H13) (Supplementary Fig. S2A).

3.2.2. 3D structure and active center analysis

The 3D structural models for Sea bass SCD 1b were obtained by homology modelling in Phyre2 Protein Fold Recognition server and SWISS-MODEL server. As target structure c4ymkA (http://www.pdb.org/pdb/explore/explore.do?structureId=4ymkA), the single highest scoring template, was used. The generated models (PDB file, supplementary material S3) shows a confidence of 100% and a coverage of 94% (315 residues) to the target in Phyre2 server and 91% and 92% respectively in SWISS-MODEL server (Fig. 4). The evaluation of the structure by Structure Assessment tools in SWISS-MODEL server, yielded an estimated global quality value QMEAN of −2.91, being Ramachandran favoured 94.39% of the residues, Ramachandran outliers 0.99% of the residues, rotamer outliers 0.39% of the residues and 1016% of bad angles (Supplementary material S4). Both models show a monomeric structure with four large trans-membrane α-helices matching with the largest α-helices observed in the secondary structure. The four TMS support the rest of the protein structure, which rests on the cytosolic face of the membrane supported on the helices H3, H12 and H13, also with a marked hydrophobic character, giving it a straight hook-like architecture (Fig. 5). Two metal ions (Fe^{2+}), essential for catalytic activity, are coordinated with nine histidine residues, forming the di-iron active center (Fig. 6A). Metal ion 1 appear coordinated to five His residues (H95, H100, H132, H136 and H276, Fig. 6B) while metal ion 2 is coordinated with four His residues (H135, H244, H273 and H277, Fig. 6C). Both models coincide in involving a new additional residue of His (H244) in the stabilization of the ferrous ions 1, previously not described in fish, and an Asn residue (N240), through a bridging ligand that could be a water molecule, completing the fifth coordination position of this metal ion (Fig. 7A, B). The distances of the coordination bonds for each of the metal ions are consistent with an octahedral symmetry for each metal atom, with the lack of a ligand in each one, which would be located between both (Fig. 7C, D).

The 3D model was analyzed using the CASTp software to locate the active center of the enzyme. The largest pocket, open to the solvent, was considered, including the tunnel in which the possible substrates are housed. The enzyme has a large cavity of 1513.0 $Å^3$, with a large opening to the solvent and an elongated tunnel, shaped like a boathook, in the hydrophobic inside of protein (Fig. 8A). A possible CoA binding site is found in the opening of the pocket (Fig. 8C). The end of the tunnel, where the fatty acid methyl group (—CH_3) should be placed, is formed by six residues: A87, V90, M232, T236, I268 and A267. This set of residues forms a pocked at the end of the tunnel, shaped as a template for a methyl group, in which the methyl group could place fixing the acyl chain, restricting its freedom of movement and delimiting the maximum size of substrate that could be housed inside and be transformed with greater efficiency (Fig. 8B). A Tyr residue in TM2, (Y83), conserved in Sea bream (*S. aurata*), in Fugu (*T. rubripes*), in all isoforms of mouse SCD (*M. musculus*) and other animals but not in other fishes SCD 1a (Fig. 1), seems to block the exit of the tunnel.

Inside the tunnel, the substrate C18:0 is housed with a conformation that places the C9-C10 bound near the Fe^{2+} ions, fixing the methyl group and restricting the movement capacity of the acyl chain (Fig. 8D). Docking analyzes show that the acyl chain could adopt different conformations inside the tunnel, positioning the C11-C12 bond at a suitable distance from the metal ions so that the *cis*-double bond could be formed (Fig. 8E, F). This particular conformation prevents the methyl of the acyl

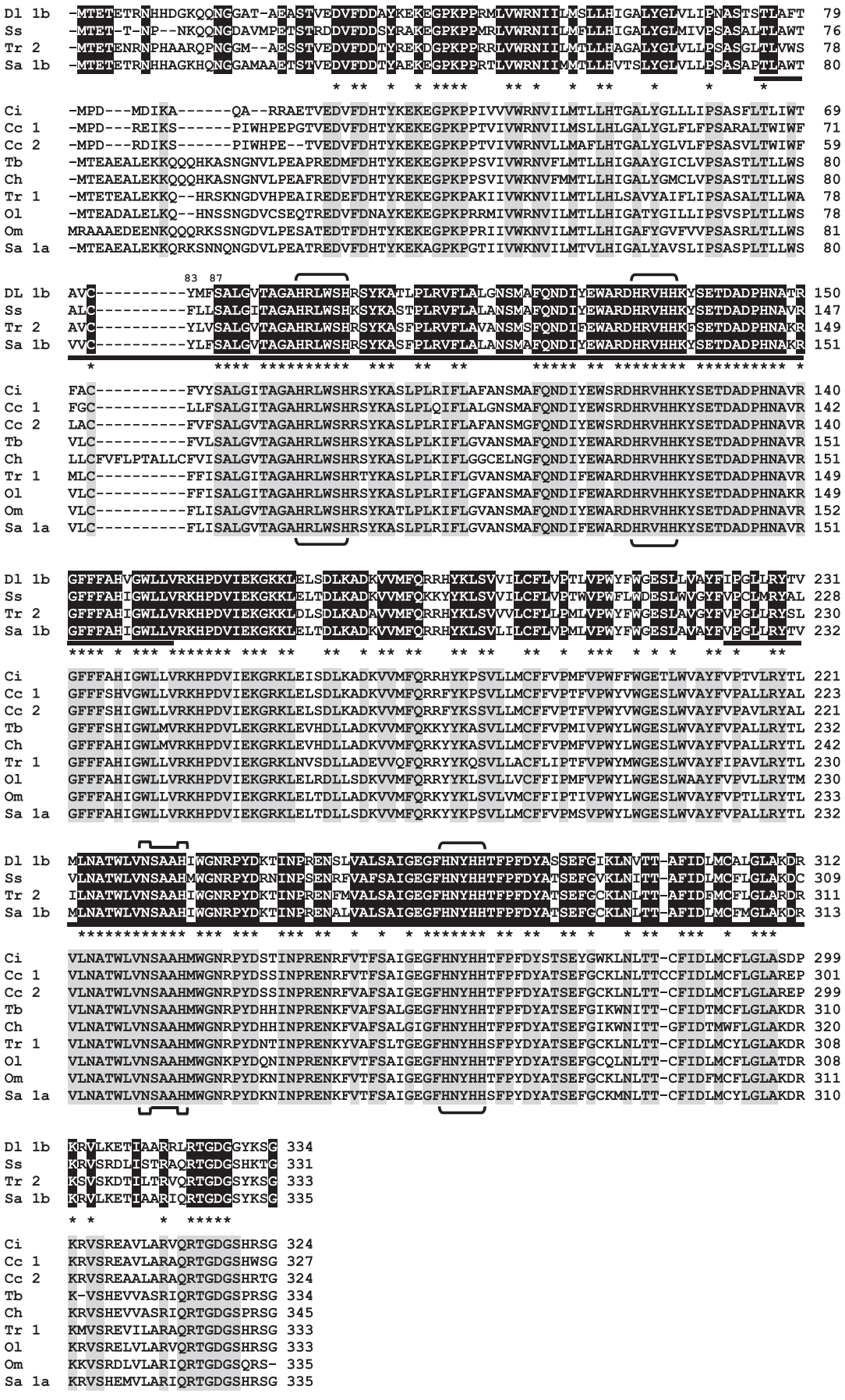

(caption on next page)

Fig. 1. A) Comparison of the deduced amino acid sequence of the European sea bass SCD 1b (Dl) (*Dicentrarchus labrax*) with SCD from Fugu (Tr) *Takifugu rubripes*, Sea bream (Sa) *Sparus aurata*, Atlantic salmon (Ss) *Salmon salar*, Grass carp (Ci) *Ctenopharyngodon idella*, Common carp (Cc) *Cyprinus carpio*, Emeral rockcod (Tb) *Trematomus bernachii*, Antarctic icefish (Ch) *Chionodraco hamatus*, Medaka (Ol) *Oryzias latipes* and Tilapia (Om) *Oreochromis mossambicus*. Protein sequences were aligned using Clustal Omega. For SCD 1b protein identical residues are shaded black. For other SCDs, conserved residues are shaded grey. (*): conserved residues in all SCDs 1a and 1b. (⌐¬): Sequences-conserved histidine cluster boxes. (⌐¬): Additional NX_3H like motive.

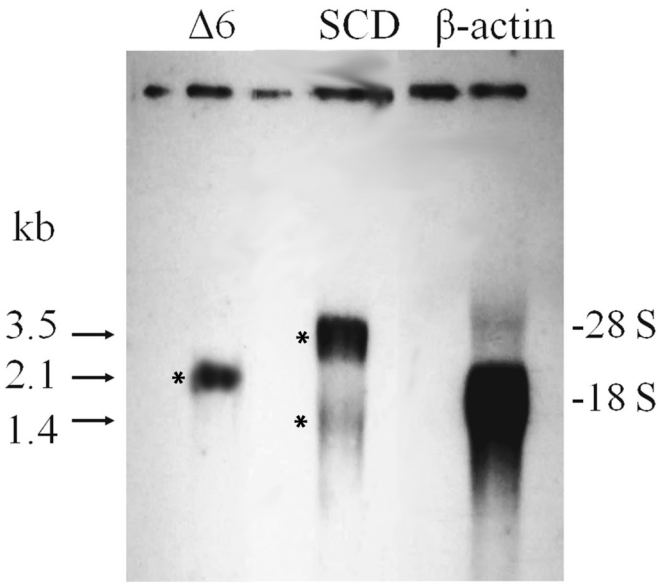

Fig. 2. Northern blot analysis of SCD mRNA from liver of European sea bass. A major band of approximately 3.5 kb was observed (*). Another minor band of 1.4 kb was observed (*). As a control, sea bass Δ6 FAD (2.1 kb) and β-actin cDNAs were used. Size of Δ6 FAD and β-actin mRNAs (2.1 kb) and ribosomal RNA 28S and 18S are indicated.

Table 2
Identity percentage among Fish and Mammals SCD and Sea bass SCD 1b.

Accession number	Scientific name	Common name	Identity (%)	SCD 1 subtype
		Fish		
CBM40644	*Dicentrarchus labrax*	European sea bass	100.0	SCD 1b
AFP97552	*S. aurata*	Sea bream	87.7	
AAU89872	*T. rubripes*	Fugu	81.3	
ACN11041	*S. Salar*	Atlantic salmon	75.8	
CAB53008	*C. idella*	Grass carp	74.6	SCD 1a
AAB03857.2	*C. carpio*	Common carp (1)	73.7	
CAB57858	*C. carpio*	Common carp (2)	73.1	
AAN77732	*O. mossambicus*	Tilapia	71.2	
XP004080473	*O. latipes*	Medaka	71.1	
AFP97551	*S. aurata*	Sea bream	70.9	
CBN81527	*D. labrax*	European sea bass	70.3	
ACI16378	*Trematomus bernacchii*	Emerald rockcod	68.8	
CAB56151	*C. hamatus*	Antarctic icefish	68.5	
AAH95851	*Danio rerio*	Zebrafish (b)	74.3	SCD 1
AAL99291	*Chanos chanos*	Milkfish	71.5	
AAO25582	*D. rerio*	Zebrafish (a)	68.9	
		Mammaliam		
AAH05807	*H. sapiens*	Human	61.9	SCD 1
AAH07474	*M. musculus*	Mouse	60.7	
AAH61737	*R. norvegicus*	Rat	59.8	

chain from occupying the pocked at the end of the tunnel and possibly increases the freedom of movement of the acyl chain inside the tunnel. However, we have not found restrictions on the minimum size of the acyl chain that could be lodged in the tunnel, beyond being an acyl chain of at least 10 carbons, and, therefore, susceptible to being transformed.

3.3. Heterologous expression in yeast S. cerevisiae

The FA profile analysis of yeast (strain INVSc1) expressing putative sea bass SCD, in absence of any substrate added to the growth medium, showed that total SCD activity, over 16:0 and 18:0 substrates, increased, after 18 h and 48 h of induction (specific conversion values of 60.25% and 63.20%, respectively), versus the total endogenous SCD activity of the control yeast (60.0% and 53.3%, respectively) (Table 3). When the medium was supplemented with 18:0 substrate, at 18 h after induction, an increase of total SCD activity, over 16:0 and 18:0 substrates, was observed compared to total endogenous SCD activity of the control yeast (48.5% vs 41.7%, respectively) (Table 4). However, 48 h after induction, total SCD activity of transformed yeast over 16:0 and 18:0 substrates decreased compared to total endogenous SCD activity showed by the control yeast (48.3% vs 50.7%, respectively). A detailed analysis shows that SCD activity over 18:0 substrate increased (23.8% vs 20.4%, respectively) while 16:0 conversion decreased (24.5% vs 30.30%, respectively) (Table 4).

3.4. Yeast complementation

We complemented the *ole1 HpaIΔ::LEU2*, DTY-11A yeast, a *S. cerevisiae* strain defective in SCD activity and MUFAs synthesis, using pD9DpYES2 plasmid containing the coding sequence for a putative Δ9 FAD of sea bass. After 96 h, transformed yeasts were able to grow at 28 °C on solid and liquid medium lacking MUFAs, indicating that the transcribed ORF sequence codes for a functional protein product in yeast, complementing the lack of SCD activity of the mutant strain. To discard possible contaminations, the FA profile of control and transformed yeast colonies grew in a solid medium, were analyzed and compared (Fig. 9). The FA profile of control yeast ($n = 2$), showed the main FAs found in *S. cerevisiae,* 12:0, 14:0, 16:0 and 18:0 (peaks 1, 2, 3 and 4, respectively), together with the exogenously added fatty acids 16:1 n-7 and 18:1 n-9 (peaks 5 and 6, respectively) (Fig. 9C). The FA profile of the two yeast clones transformed with the plasmid pD9DpYES2 grew in the absence of the MUFAs, showed the peaks 16:1 n-7 (peak 5) and 18:1 n-9 (peak 6), corresponding to the Δ9 desaturation products of 16:0 and 18:0, respectively (Fig. 9A and B). These peaks were less prominent than those observed in yeast used as control (Fig. 9C). All peaks were assigned as is described previously. As mean, 4.86 ± 0.19% of 16:0 was converted to 16:1 n-7 and a 9.0 ± 0.46% of 18:0 was converted to 18:1 n-9, being 13.86 ± 0.65% the total specific SCD conversion estimated in yeast transformed with the pD9DpYES2 plasmid (Table 5).

3.5. Genes expression of scd1b and Δ6 fad in European sea bass tissues

The *scd1b* and *Δ6 fad* transcription in Sea bass tissues (brain, heart, gonad, liver, adipose tissue and intestine) were monitored by quantitative PCR analysis. The absolute expression level was expressed as the mean number of molecules in 25 ng of total RNA (± SEM) from five individuals. *Scd 1b* and Δ6 *fad* genes were transcribed in all examined tissues. Liver and adipose tissue showed the highest levels of SCD 1b

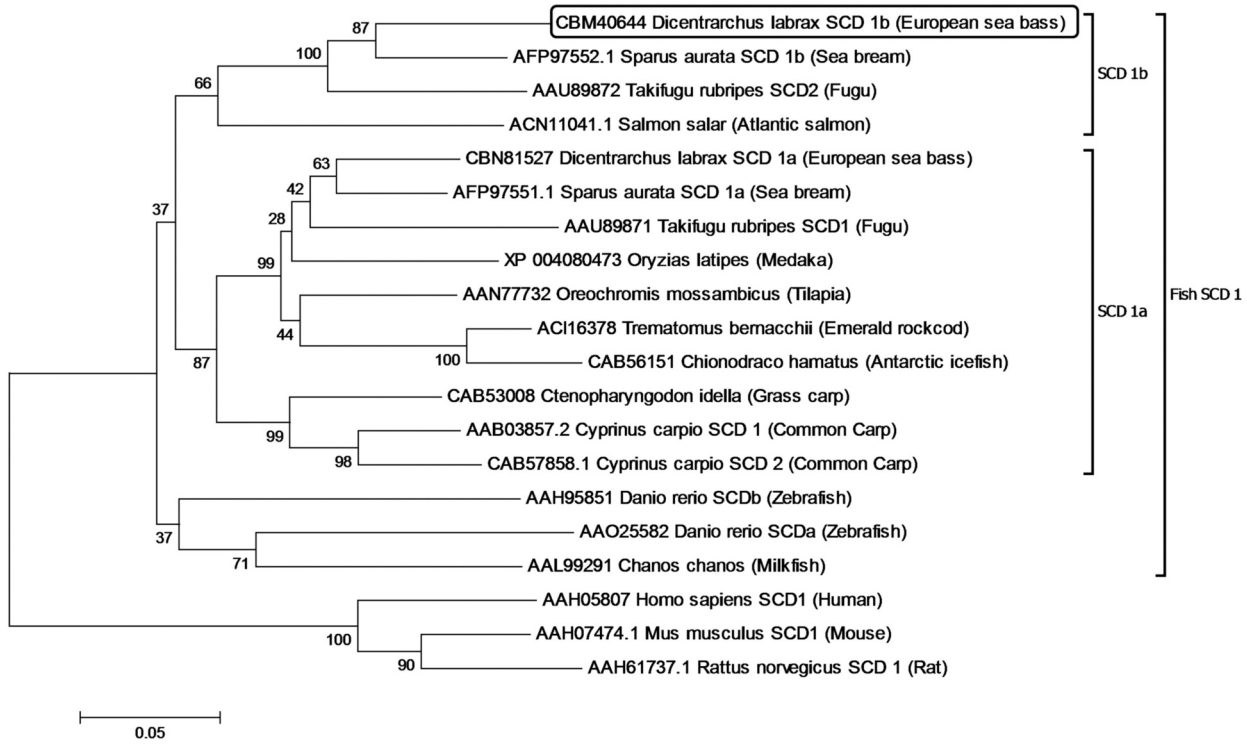

Fig. 3. Evolutionary relationships of taxa. Phylogenetic tree comparing putative amino acid sequences of European sea bass SCD 1b with other SCD sequences from fishes, constructed by Neighbor-joining (NJ) method. The percentage of replicate trees in which the associated taxa clustered together in the bootstrap test (1000 replicates) is shown next to the branches (Felsenstein, 1985). The tree is drawn to scale, with branch lengths in the same units as those of the evolutionary distances used to infer the phylogenetic tree. The evolutionary distances were computed using the p-distance method and are in the units of the number of amino acid differences per site. The analysis involved 20 amino acid sequences. All positions containing gaps and missing data were eliminated. There were 312 positions in the final dataset.

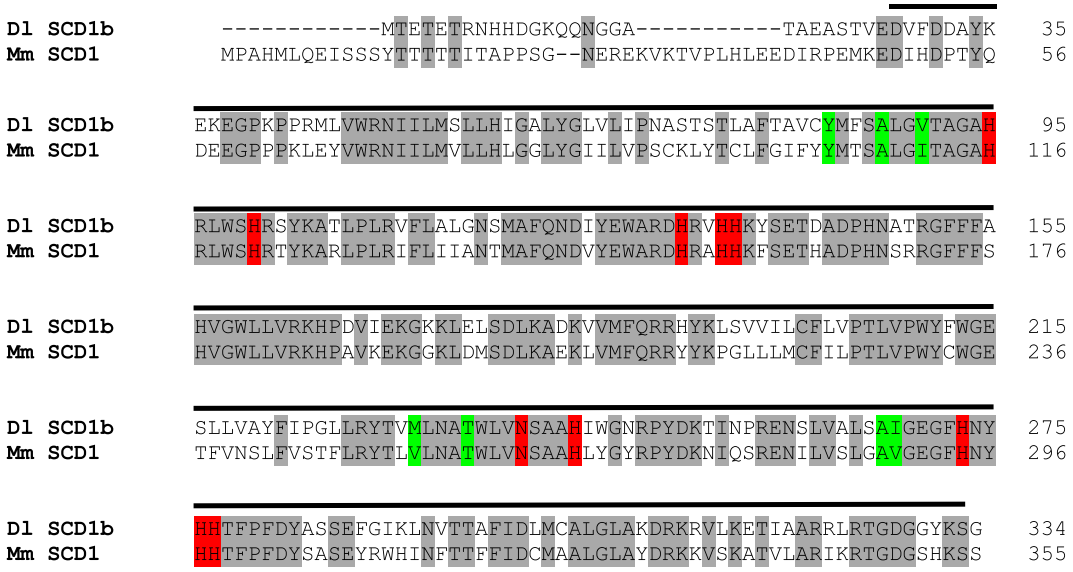

Fig. 4. Comparison of the amino acid sequence of European sea bass SCD 1b (*Dicentarchus labrax*) (Dl SCD 1b) and mouse SDC 1 (*Mus musculus*) (Mm SCD 1). Identical amino acids in both sequences are shown shaded. The amino acids involved in the coordination of the metal atoms are shaded in red. Shaded in green are the amino acids, previously described, involved in blocking the end (Tyr83 and Ala87 in Fig. 1) of the tunnel in which the substrates are housed. Other amino acids, possibly involved in form the pocked at the end of the tunnel, are also shaded in green. The black line shows the region of the mouse SCD protein that has been used to model the 3D structure of the European sea bass protein. (For interpretation of the references to colour in this figure legend, the reader is referred to the web version of this article.)

mRNA. Brain, gonad and heart exhibited a similar transcription level and considerably lower than liver or adipose tissue. Intestine showed the lowest expression level (Fig. 10A). The transcription of *Δ6 fad* gene was highest in brain, showing gonad, heart, intestine, adipose tissue and liver a smaller level. In all analyzed tissues, transcription of *scd 1b* gene was always higher than that of Δ6 *fad* gene, as reflect SCD/Δ6 FAD

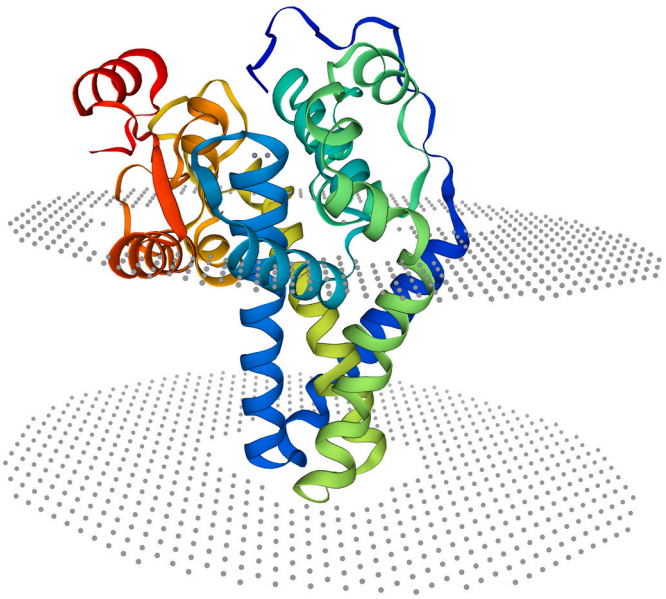

Fig. 5. 3D modelling of the deduced protein. 3D structure was modelled using Swiss-Model server. Template protein 4ymkA.1 was selected for homology modelling. Four large transmembrane α-helices attach the protein to the membrane of the endoplasmic reticulum, giving it a straight hook-like architecture.

relative transcription ratio (RTR) values (Fig. 10B).

3.6. Subcellular localization of cDNA proteic product

DLEC cells were co-transfected with pSCD1b/EGFP and pDsRed2-ER to determine the subcellular localization of SDC1b-EGFP (green fluorescence) and to specifically mark the endoplasmic reticulum (ER) (red fluorescence). At 72 h, green fluorescence was observed with a diffuse cytoplasmic distribution and a marked perinuclear pattern, clearly suggesting an ER pattern (Fig. 11B). Red fluorescence, designed to specifically localize ER, showed a pattern highly similar to green fluorescence (Fig. 11A). Assessment of the co-localization of both signals indicated a high degree of coincidence of the green and red fluorescence, suggesting that SCD 1b is located in the ER (Fig. 11C). All the used indices show a high degree of co-localization of both signals (Fig. 11), what confirms the location of the sea bass SCD 1b in the endoplasmic reticulum.

4. Discussion

Fatty acid desaturation, in which several enzymes of the FAD superfamily with different substrate specificities and regio-selectivity participate, is a highly complex and regulated process. The products of these activities are key components of membrane phospholipids, triglycerides, cholesterol esters and wax esters, playing an important role in the energy storage and production, maintenance of the physiological properties of membranes, and as signalling molecules (Paton and Ntambi, 2009). The maintenance of an appropriate unsaturated/saturated fatty acids ratio assures the correct operation of the cellular membranes as well as the cellular signalling system in which they are involved (Flowers and Ntambi, 2008). Although this ratio mainly depends of the diet, desaturase enzymes play an important shock paper, possibly indicating that the expression and function of the different FADs are a highly coordinated process. In this context, we aim to study how the complex system of fatty acid desaturation is regulated/coordinated in marine fish. Previously, we had cloned and characterized a Δ6 FAD cDNA from European sea bass (González-Rovira et al., 2009) and, in the present work, an SCD 1b cDNA, a second member of this desaturation complex system, was obtained and in silico and functionally characterized.

4.1. Cloning and sequence analyses of full-length cDNA for SCD of European sea bass

We have obtained an SCD cDNA which included all characteristics features of a full length mRNA. The 5′ region of cDNA proved to conserve sequences related to the control of the gene expression. A CT repeat element (Kenyon and Craig, 1999) and two additional *cis*-regulatory non-palindromic putative NRL-response elements (NRE), with the consensus sequence (TGC(N_{3-4})GCA), were present in this region. A wide and variated number of mechanisms, including transcriptional and translational controls (Kandasamy et al., 2004), regulates the *scd* gene. The existence of these three elements in the 5′-region is of considerable interest from a point of view of the regulation of the expression. All these elements are directly implied in the control of the transcription, being able to produce an up-regulation of the genes in those they are present (Kenyon and Craig, 1999; Kerppola and Curran, 1994) and, in this sense, they may be implicated in controlling *scd1b* gene transcription and thus modulate its expression. No similar *cis*-acting elements were found in sea bass Δ6 FAD cDNA.

However, translation also appears to play an important role in governing the decay of some transcripts. The decay rate of several regulated transcripts is controlled by AU-rich elements (AREs) located within the 3'-UTR (Stukey et al., 1990; Vemula et al., 2003). AREs are also present in a wide variety of genes as *ole 1* of *S. cerevisiae* (Vasudevan and Peltz, 2001; Veyrune et al., 1997), Interferons (Savan, 2014), Toll-like

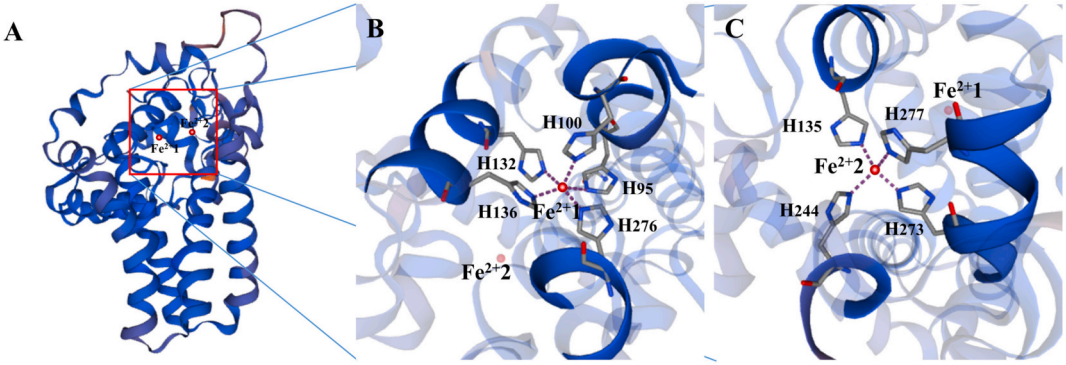

Fig. 6. A) Two Fe^{2+} metal ions are located in the active site of the enzyme (Fe^{2+}, red spheres) coordinated with nine histidine residues highly conserved. B) One of the ferrous ions ($Fe^{2+}1$) is coordinated with five histidine residues (His 95, 100, 132, 136 and 276). C) The second $Fe^{2+}2$ ion is coordinated with four histidine residues (His 137, 244, 271 and 277). (For interpretation of the references to colour in this figure legend, the reader is referred to the web version of this article.)

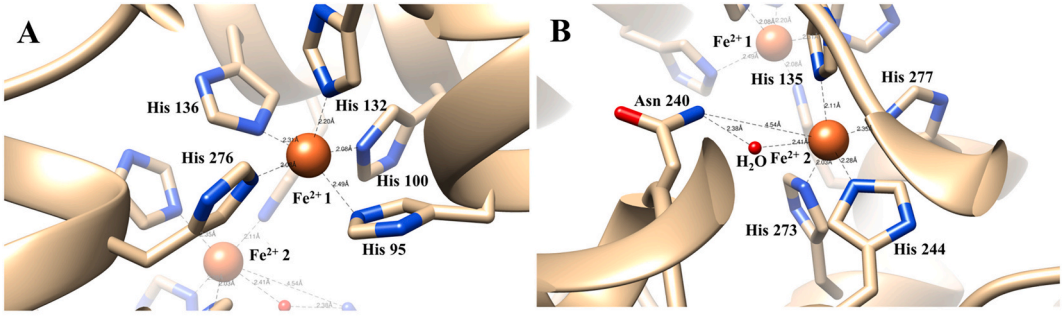

C

Atom 1	Atom 2	Distance (Å)
Fe^{2+} 1	His 95	2.49
	His 100	2.20
	His 132	2.08
	His 136	2.31
	His 276	2.08
	Fe^{2+} 2	6.39

D

Atom 1	Atom 2	Distance (Å)
Fe^{2+} 2	His 135	2.11
	His 244	2.28
	O (H_2O)	2.41
	His 273	2.03
	His 277	2.35
	N (Asn 240)	4.54
N (Asn 240)	O (H_2O)	2.38

Fig. 7. Two metal ions present in the active site are coordinated with nine histidine residues, forming the di-iron active center. Metal ion 1 appear coordinated to five His residues (A) while metal ion 2 is coordinated with four His residues and an Asn residue (N240), through a bridging ligand that could be a water molecule (B). The distances of the coordination bonds for each of the metal ions are consistent with an octahedral symmetry for each metal atom (C y D) with the lack of a ligand in each one.

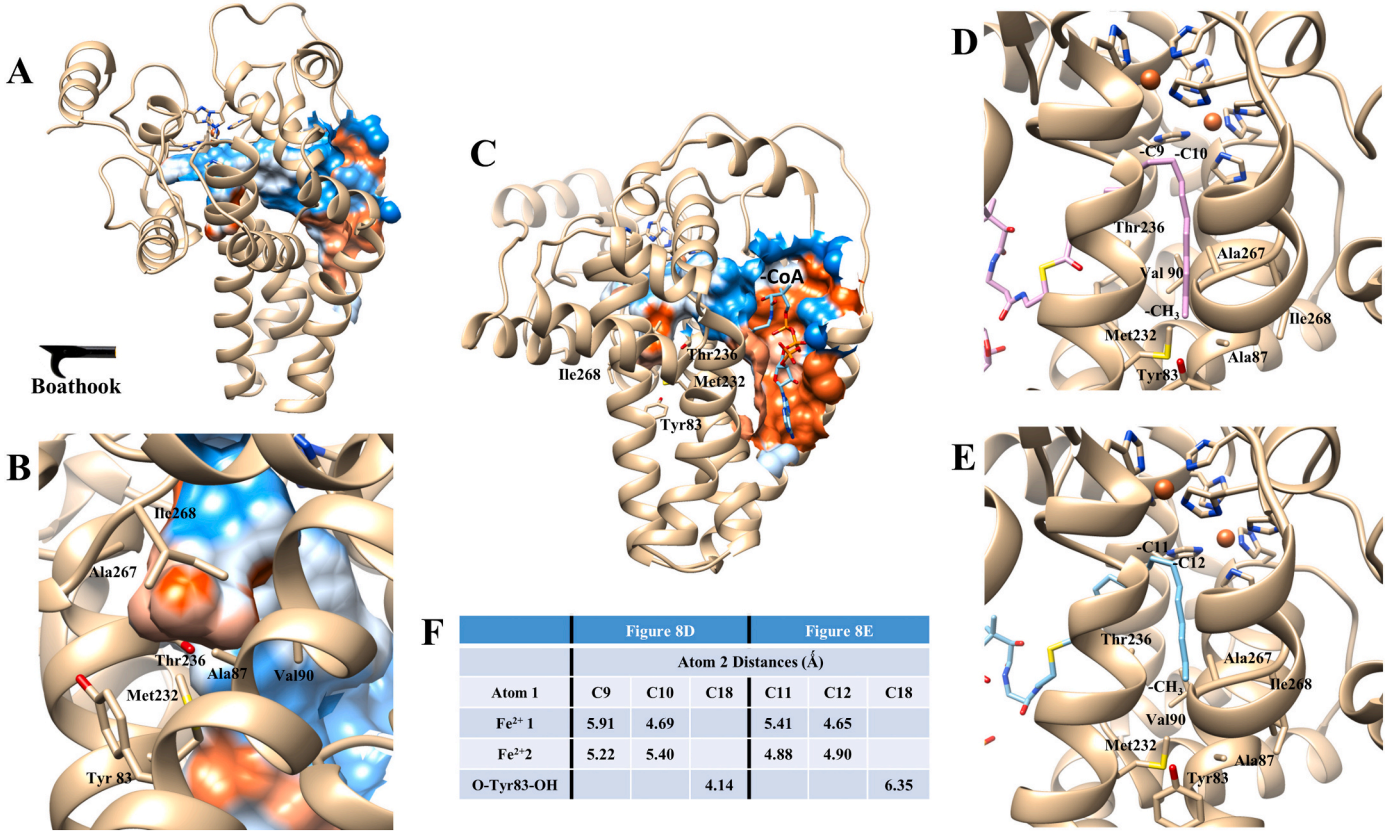

F

	Figure 8D			Figure 8E		
	Atom 2 Distances (Å)					
Atom 1	C9	C10	C18	C11	C12	C18
Fe^{2+} 1	5.91	4.69		5.41	4.65	
Fe^{2+}2	5.22	5.40		4.88	4.90	
O-Tyr83-OH			4.14			6.35

Fig. 8. Active site of the enzyme. The CASTp server was used to locate the active site. Figures and distances were obtained with UCSF Chimera 1.15 software. The pocket with the largest volume was chosen. A) Active site of the enzyme corresponding to the largest pocket. The hydrophobic regions appear colored in blue and colored in red the hydrophilic regions. The sharply kinked pocket, whose external appearance is reminiscent of a boathook, has a large mouth area, exposed to the solvent and long, narrow and highly hydrophobic tunnel, into which the different substrates are fits. B) The end of the tunnel is formed by seven amino acids that are facing toward the tunnel and located in different α-helices of the protein: Y83, A87, V90 (TM2); M232, T236 (TM3); A267 and I268. The pocket at the end of the tunnel is shaped like a template for the methyl group, suggesting to be a point of attachment for the C18 of the acyl chain. C) CoA binding site in the mouth area, the most exposed to the solvent region of the active site. D) Position of the 18-carbon acyl chain inside the tunnel. The C9-C10 bond is arranged inside the tunnel, near the Fe^{2+} metal ions. In this conformation of the acyl chain, the methyl group is positioned in the final pocket of the tunnel. E) An alternative conformation, obtained by Docking analysis, shows how the C11-C12 bond of the acyl chain is positioned in a similar site to that occupied by the C9-C10 bond in D). The methyl group is further away from the end pocket of the tunnel. F) Interatomic distances in the two conformations D) and E) of the acyl chain. While the distance of each of the metal ions to the C9 and C10 carbons in D) and C11 and C12 carbons in E) is maintained, the distance between C18 and oxygen of the -OH group of Y83 is higher in E). (For interpretation of the references to colour in this figure legend, the reader is referred to the web version of this article.)

Table 3
Functional characterization of Sea bass SCD 1b cDNA in INVSc1 yeast strain.

Without substrate (18:0) added				
	$t = 18$ h		$t = 48$ h	
Fatty acids	Control (%)	Induction means value (%)	Control (%)	Induction means value (%)
16:0	28.30 ± 0.15	29.60 ± 0.20	35.30 ± 1.80	27.70 ± 1.60
16:1	34.10 ± 0.00	29.20 ± 1.50	28.10 ± 2.40	31.05 ± 0.15
18:0	11.80 ± 2.05	10.00 ± 1.10	11.10 ± 1.05	9.00 ± 0.20
18:1	25.90 ± 0.10	31.05 ± 0.15	25.20 ± 3.10	32.15 ± 1.35
SCD specific conversion	60.00 ± 0.10	60.25 ± 1.65	53.30 ± 5.50	63.20 ± 1.50

Values (% of peak area) are means of the indicated numbers of replicated (n) with standard deviation. (n=2)

Table 4
Functional characterization of Sea bass SCD 1b cDNA in INVSc1 yeast strain.

With substrate (18:0) added				
	t = 18 h		t = 48 h	
Fatty acids	Control (%)	Induction means value (%)	Control (%)	Induction means value (%)
16:0	17.90 ± 0.10	24.20 ± 0.50	25.50 ± 2.10	20.90 ± 1.30
16:1	23.80 ± 0.90	25.10 ± 2.00	30.30 ± 0.30	24.50 ± 0.10
18:0	40.30 ± 2.10	27.25 ± 4.95	23.80 ± 2.30	30.80 ± 1.70
18:1	17.90 ± 1.10	23.40 ± 2.50	20.40 ± 0.15	23.80 ± 0.60
SCD specific conversion	41.70 ± 2.00	48.50 ± 4.50	50.70 ± 0.45	48.30 ± 0.70

Values (% of peak area) are means of the indicated numbers of replicated (n) with standard deviation. (n=2)

receptor 22 of gilthead sea bream (Muñoz et al., 2014), as well as in other members of the fatty acids desaturation system, including European sea bass Δ6 FAD, being a broadly extended mechanism of translational control of *scd* genes (Ntambi, 1999). Surprisingly, no AREs are present within the 3'-UTR of Sea bass SCD 1b cDNA, in contrast to other members of the FAD system, which have AREs in the 3'-UTR region. Thus, Sea bass Δ6-FAD cDNA (GenBank accession no. **AM746703.1**) has two AREs and Sea bass Elovl5 cDNA (GenBank accession no. **FR717358.1**) has three AREs, located in the same region. The absence of AREs in the SCD1b mRNA suggests that the regulation of their expression in sea bass is not governed by the decay rate of mRNA, in opposition to what could happen to *Δ6 fad* or *Elovl5* genes and, taken together with the presence of other *cis*-acting regulator elements in the 5'-UTR region, could explain the high levels of specific SCD 1b mRNA detected in all tested tissues versus to Δ6 FAD mRNA levels.

At the 3'-UTR did not found the standard poly-A signal (AATAAA), although alternatives and overlapped poly-A signals (CATAAA, AATATA and TATAAA) were found. The presence of several alternative poly-A signals may lead to more than one transcript from the same gene. Accordingly, Northern blot analysis of total RNA from the liver of three individuals showed the presence of two possible transcripts, with an estimated size of 3.5 kb and 1.4 kb. The presence of two transcripts could be explained by the existence of two paralog *scd* genes in the genome, due to the whole genome duplication event that occurred early in vertebrate evolution or, also, due to an alternative splicing process by the usage of alternative poly-adenylation signals. Two *scd* gene types, *scd1* and *scd5*, are present in vertebrates due to an ancient duplication event, codifying enzymes that display similar Δ9 desaturation activity but showing different expression patterns (Paton and Ntambi, 2009). However, the *scd* genes present in teleost fish exclusively belong to the *scd1* type (Castro et al., 2011), although some teleost species have multiple SCD isoforms (*scd 1a* and *scd 1b*) due to a recent genome duplication event (3R) in teleost (Evans et al., 2008; Castro et al., 2011; Wu et al., 2013). In addition, alternative splicing should be taken in consideration. Thus, two SCD transcripts from a unique gene, with a size of 3.9 and 5.2 kb, were found in humans, due to the usage of tandem poly-adenylation sites (Zhang et al., 1999). Therefore, the casuistry are wide.

For Sea bass SCD both, the presence of two *scd1* genes and/or the occurrence of alternative splicing of the same gene, could be considered. Thus, in GenBank database, it is present a *D. labrax* genomic DNA sequence from chromosome 1 (GenBank accession no. **CBN81527.1**), from which a putative SCD 1a is deduced. This putative enzyme shows greater homology with other SCD 1a than SCD 1b enzymes (Table 2), which supports the idea that at least two *scd1* genes are present in the sea bass genome, corresponding to an SCD 1b subtype the SCD cDNA obtained in this work. On the other hand, we cannot discard the idea that more than one transcript from one or two *scd* genes could be present in Sea bass transcriptome, due to the usage of tandem poly-adenylation sites, being the cDNA obtained in this work the result of this process. In this sense, other species, like grass carp (GenBank accession no. **AJ243835**), have a 3′-UTR of SCD mRNA of great size, in human, a unique gene produces two transcripts and for sea bass SCD 1b cDNA alternatives and overlapped poly-A signals are present in the 3′-UTR. Taking into consideration all the above, we assume that the cDNA obtained in this work corresponds to a transcript of an *scd 1b* gene that shows alternative splicing in its 3′-UTR. This statement is endorsed also by the result of the Northern blot analysis, using high astringency conditions, in which a transcript of 3.5 kb is mainly appreciated.

The cDNA encoded a protein of 334 aa what shares a high percentage of identity with other fish SCD 1b previously reported (Table 2). According to that, the phylogenetic analysis places Sea bass SCD in the same branch as other modern teleost fish SCD 1b. The predicted amino acid sequence possesses three conserved histidine motifs, including eight residues of His. Together with a ninth His residue external to these motifs, they are involved in the binding of metallic ions. Its function has been demonstrated to be necessary for the protein activity, binding iron ions that participate in the catalytic activity of the enzyme (Aki et al., 1999; Cho et al., 1999a, 1999b; Leonard et al., 2000; Marquardt et al., 2000; Napier et al., 1998; Shanklin et al., 1994; Watts and Browse, 1999; Bai et al., 2015; Shen et al., 2020). All His residues are located on the cytoplasmic side of the endoplasmic reticulum (Chang et al., 2001; Hsieh et al., 2001, 2003, 2004). The ninth additional histidine residue, has previously been described in mammals (Bai et al., 2015; Shen et al., 2020), but is nevertheless also present and appears conserved in the same relative position in all SCD 1b and 1a of all fish species analyzed in this work. In silico analysis showed that, the deduced protein has a membrane-FAD-like superfamily domain, including two SCD subdomains. The protein has six highly hydrophobic segments, three of which would be capable of being included across the reticulum membrane for a total of four times, being both *N*- and *C*-termini of the enzyme facing the cytosol. This topology would group all the histidine boxes, the ninth additional His and the N-terminal and C-terminal ends in the same face of the endoplasmic reticulum membrane, the cytosolic side. This protein membrane topology has been previously proposed for other SCD, as the mouse (Weng et al., 2006), rat (Stukey et al., 1990), *L. gooser* (Zhang et al., 2013), a marine copepod *C. hyperboreus* (Meesapyodsuk and Qiu, 2014) and for a Δ6 FAD from *D. labrax* (González-Rovira et al., 2009).

The 3D models generated using the Swiss-Model and Phyre2 servers show a high degree of confidence and coverage. Two metal atoms are housed in the cytosolic region of the structure that corresponds to the Ferrous ions (Fe^{2+}) essential for enzymatic activity. The coordination geometry of both ions is compatible with an octahedral symmetry, in

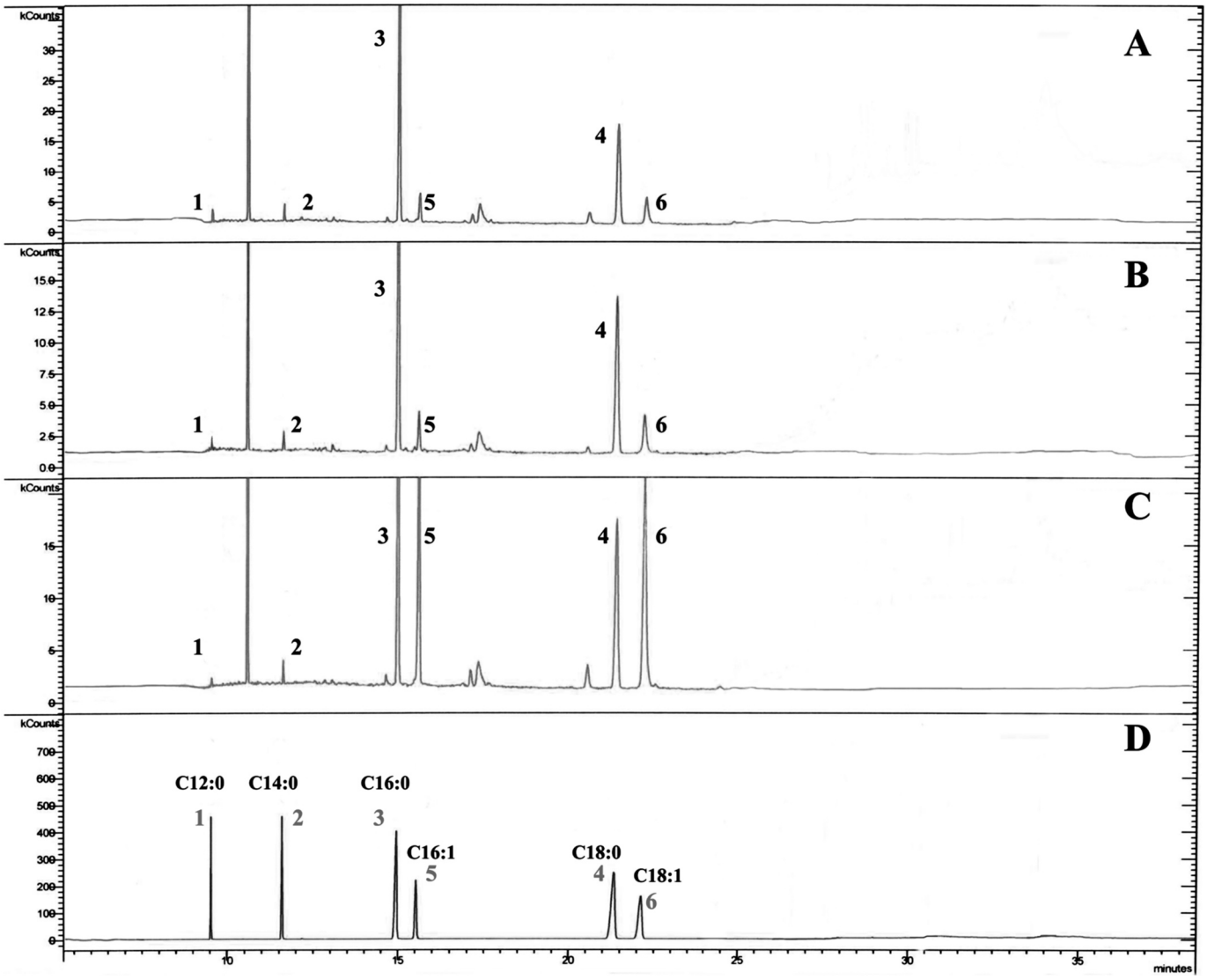

Fig. 9. Functional characterization of the putative European sea bass SCD by heterologous expression in yeast (*Saccharomyces cerevisiae*) strain ole1 HpaIΔ::LEU2, DTY-11A. Panels A and B show the fatty acid profiles obtained from yeast transformed with pYES vector containing the putative European sea bass SCD 1b insert and grown in absence of fatty acids 16:1 n-7 and 18:1 n-9 in the medium. Panel C shows the fatty acid profile obtained by GM-LC from yeast transformed with empty pYES vector, expression induced and grown in the presence of 16:1 n-7 and 18:1 n-9. Panel D corresponds with a fatty acids pattern used as a reference for unequivocally identify the correct fatty acids. Numbers in red in panel D mark fatty acids identified in panels A, B and C. Peaks 1, 2, 3 and 4 are the main fatty acids of *S. cerevisiae*, 12:0, 14:0, 16:0 and 18:0, respectively. In panels A) and B), peaks 5 and 6 were identified as the resultant desaturase products from peaks 3 and 4 respectively. In panel C, peaks 5 and 6 are 16:1 n-7 (5) and 18:1 n-9 (6) fatty acids exogenously added to the medium. Vertical axis: kCounts; horizontal axis: retention time. (For interpretation of the references to colour in this figure legend, the reader is referred to the web version of this article.)

Table 5
Yeast complementation of SCD 1b cDNA in SCD defective DTY-11A yeast strain.

Fatty acid	DTY-11A strain (control) (%)	Δ9–11 clon (%)	Δ9–17 clon (%)	SCD specific conversion: mean value ± SD (%)
16:0	30.09	52.82	53.31	
16:1	20.22	5.00	4.72	4.86 ± 0.19
18:0	20.53	32.84	33.30	
18:1	29.16	9.33	8.67	9.00 ± 0.46
Total	100	100	100	13.86 ± 0.65

Values correspond to % of specific peak area of the four fatty acids analyzed.

which a ligand is missing in the vertices located between both metal atoms in their respective octahedron. Thus, one of the Ferrous ions appears coordinated with five His residues. However, the second ferrous ion appears coordinated with only four His residues. A water molecule would coordinate the fifth position, which in turn would be coordinated with an asparagine residue through a hydrogen bond. We agree that the Asn240 residue in TMS4 would play this role as previously described (Bai et al., 2015; Shen et al., 2020). Both Asn240 and His244 belong to a motif of the NX_3H like, which is conserved in SDC1a and 1b in fish and mammals (Bai et al., 2015) and is symmetrically equivalent to the HX_4H motif that interacts with the first ferrous ion. The model is built using the c4ymkA structure as a target. Thus, the distance between the two metal ions is 6.39 A, which is greater than that found in any resolved structures of other metalloenzymes containing a di-iron active site. These enzymes use non-heme di-iron active sites with His and carboxylate ligands (Jasniewski and Que Jr., 2018). As in the target, in the sea bass SCD 1b active site the metal ions are coordinated by nine His and a putative water molecule, but in their close environment, no carboxylate residues are located that allows bidentate coordination with the metal atoms. These properties of the di-iron center, as proposed by Bai et al. (2015) and later Shen et al. (2020), suggest that the activation of molecular

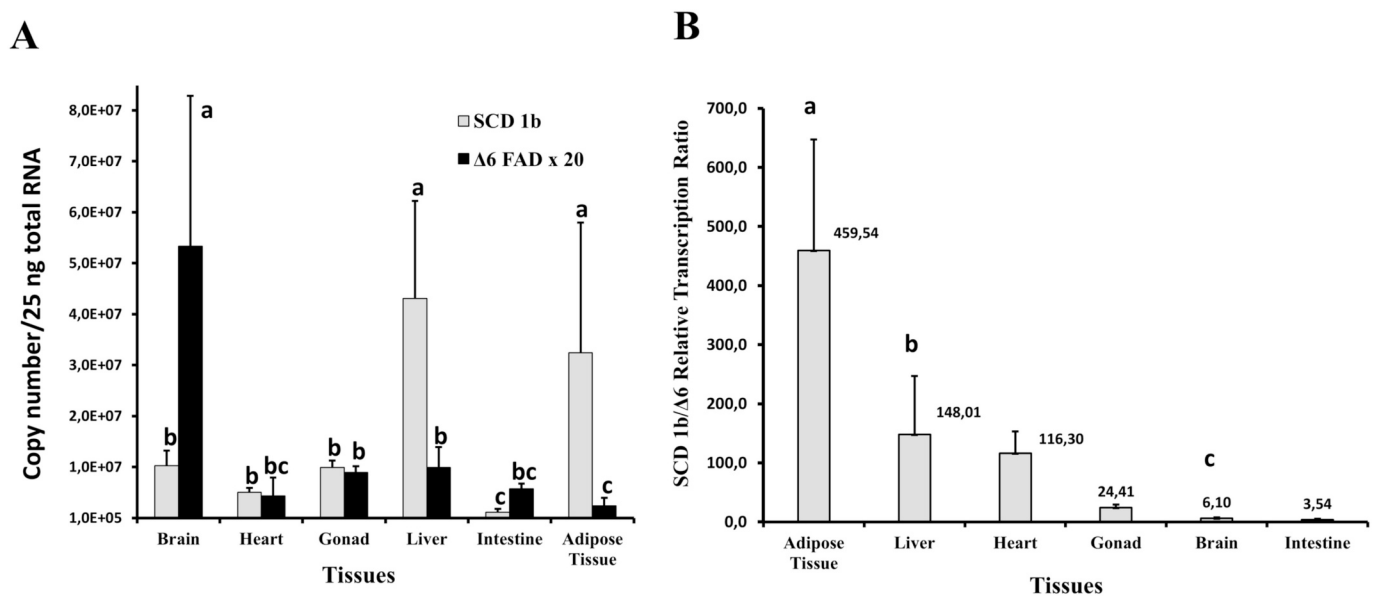

Fig. 10. Tissue transcription profile of *scd 1b* and *Δ6 fad* genes in European sea bass. A) Relative (ΔC_T) transcription levels were determined by Real Time quantitative PCR (RT-qPCR) as described in the Materials and Methods section. Results are expressed as means ± SEM ($n = 5$). Different superscript letters (without accent for SCD 1b transcription and with accent for Δ6 FAD transcription) show significant differences among tissues ($p < 0.05$). B) SCD/Δ6 FAD relative transcription ratio (RTR). For each individual, the ratio between the transcription of SCD and Δ6 FAD for each tissue was calculated. Results are expressed as means (±SEM) (n = 5).

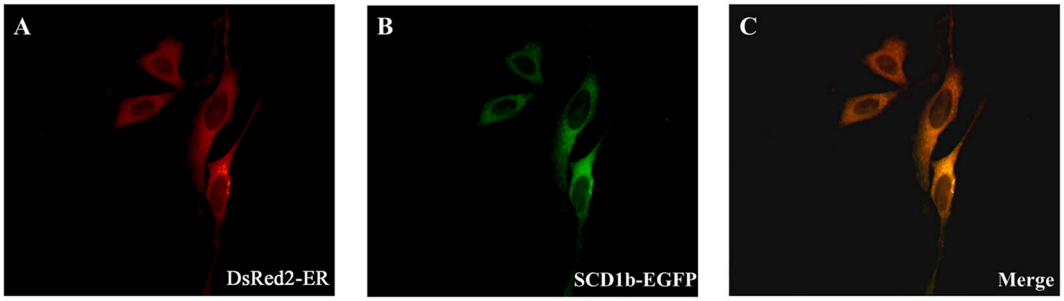

Quantitative Colocalization (n=10)		
Pearson's (-1.0,1.0)	Overlap (0.0,1.0)	Li's ICQ (-0.5,0.5)
0,83 ± 0,06	0,97 ± 0,01	0,34 ± 0,13

Fig. 11. Subcellular localization of SCD 1b from European sea bass in DLEC line. The plasmid coding for the fusion protein SCD 1b-EGFP was transiently co-transfected into cells with pDsRed2-ER, a commercial plasmid designed to localize the endoplasmic reticulum. Forty-eight hours after transfection, red channel (panel A) and green channel (panel B) fluorescent images were taken for the same field. Overlay composed of two channels (panel C) shows in yellow pixels where the red and green channels match. To quantify the degree of co-localization, intensity correlation coefficient-based (ICCB) analyses were performed, using JACoP tool included in Image J software (v. 1.42 k) (http://rsb.info.nih.gov/ij). In D), Pearson's and Overlap coefficients and Li's Intensity Correlation Quotient (ICQ) for ten analyzed images, are shown as mean ± SD. Maximum (completed co-localization) and minimum (exclusion) values for each coefficient are indicated. All estimates were made on a set of 10 fields ($n = 10$). (For interpretation of the references to colour in this figure legend, the reader is referred to the web version of this article.)

oxygen in SCD1b could occur through a new mechanism. Thus, our 3D model reinforces this hypothesis.

4.2. Heterologous expression in yeast S. cerevisiae, yeast complementation and subcellular localisation

To functionally characterize SCD enzyme from European sea bass, we have performed two assays in a heterologous expression system, using two different *S. cerevisiae* yeast strains. A third subcellular localization assay has been developed in a homologous system. On one hand, we have demonstrated that the transcribed ORF sequence coded for a functional protein that complemented the lack of Δ9 FAD activity of the *ole1 HpaIΔ::LEU2*, DTY-11A mutant yeast strain, indicating that is a SCD enzyme. In this assay, the enzyme showed a higher preference in the transformation of 18:0 substrate (9.0%) than 16:0 substrate (4.9%) (Table 5). However, it is important to have in consideration that the enzyme showed a low conversion capacity in this heterologous system. This can be due to several causes, as that the expression is carried out in a heterologous system, the temperature to which is carried out the assay can influence the activity, and that this protein lacks a cytochrome *b*5 domain, that it is present in the OLE1 yeast enzyme, among others. All they can be decisive so that the enzyme shows a low conversion capacity. González-Rovira et al. (2009) equally describe a low capacity of conversion of the Δ6 FAD when it was functionally characterized in yeast. On the other hand, we tested the SDC activity in INVSc-1 yeast strain in absence and presence of exogenously supplemented 18:0 substrate. In absence of 18:0 substrate, the enzyme showed a higher preference for 18:0 than for 16:0, as has been previously noted by Stukey et al. (1990) and Meesapyodsuk and Qiu (2014). The highest preference of the enzyme for the FA with more carbons is a general characteristic of

fatty acyl desaturases (Stukey et al., 1990; Tocher et al., 1998). Likewise, when the medium was supplemented with 18:0 as substrate (stearic acid), SCD activity showed an increase, after 18 h of induction, compared to the control yeast (Table 5). This increase was due to the increment of the conversion of both 16:0 and 18:0 substrates. However, after 48 h of induction total SCD activity showed a decrease versus control yeast (Table 4). This decrease was mainly due to the lower conversion of 16:0 substrate, whereas the 18:0 conversion increased. The reason for this fact is unclear. In our opinion, this effect could be due to three causes that converge at the same time. First, as previously we indicated, the enzyme shows a very low SCD activity in the yeast. Second, due to an effect of the competition of the substrate for the enzyme in a rate-limiting context of the enzyme, since being the medium supplemented exogenously, the 18:0 substrate is in more quantity than the 16:0 endogenous substrate. Third, the biggest preference showed by sea bass SCD to transform the 18:0 than the 16:0 substrates. Therefore, we concluded that sea bass cDNA cloned in this work codes a Δ9 FAD and, when it was expressed in yeast, it showed a higher preference toward 18:0 than to 16:0 substrate. This is the first time that the full functional characterization of SCD from a marine fish has been achieved.

To fully characterize SCD 1b protein we have determined its subcellular localization. The protein coded by the cDNA showed an unequivocally SCD desaturase activity when it was assayed in a heterologous system. However, these assays do not report information about its subcellular localization, which should be the ER. Transient expression of the fusion protein SDC 1b-EGFP in the cell line of Sea bass DLEC indicates no doubt that is located in the ER, as confirmed by all evaluated co-localization indices. To our knowledge, this is the first time this determination has been done in a homologous system.

4.3. Substrate preference and specificity of sea bass SCD 1b

SCD 1 is an enzyme with a wide capacity to desaturate fatty acids of different lengths, showing a greater preference for 18C substrates (Stukey et al., 1990; Meesapyodsuk and Qiu, 2014; Miyazaki et al., 2006; Tocher et al., 1998). What is the ultimate explanation that can justify this preference? The availability of a 3D model has allowed us to study this question. The length of the tunnel limits the largest substrate that the enzyme can desaturate. In our model, seven residues form the pocket at the end of the tunnel. A Tyr residue, highly conserved in animals, has been proposed to play an important role in determining the length of the substrate (Bai et al., 2015). In Sea bass SCD 1b, the conserved Tyr 83 (on TM2) seem to have that role. The existence of this pocket, on the one hand, constitutes a steric impediment, limiting the maximum size of substrates that can be transformed. However, the minimum substrate size does not appear to be limited, although the efficiency of enzyme transformation decreases with the size of the substrate (Miyazaki et al., 2006). On the other hand, it is an attachment point for the end of the acyl chain, restricting its freedom of movement and favoring the maintenance of the C9-C10 bound in the correct position for desaturation. This justifies the greater preference for 18C substrates.

Enzyme-substrate docking analyzes show that the acyl chain can adopt conformations that allow to form the *cis*-double bond between C11-C12 carbons. Then, the desaturation product is the *cis*-vaccenic acid (C18:1 n-7). This enzymatic activity has been previously reported for mouse SCDs, although with a low efficiency (Miyazaki et al., 2006). The fact that the acyl chain can adopt different conformations inside the tunnel suggests that the volume of the tunnel is greater than that of the substrate. Therefore, the substrate could have a certain degree of freedom of movement within the tunnel. This freedom should be greater the smaller the acyl chain is and vice-versa. Likewise, larger fatty acids could also be transformed, although with low efficiency. Thus, Miyazaki et al. (2006) showed that mouse SCD 1, 2 and 4 transform C19:0 with less efficiency than C18:0.

The binding of CoA to its binding site outside the pocket and the fixation of the methyl group to the pocket at the end of the tunnel, place the bound C9-C10 near the Fe^{2+} ions, where the *cis*-double bond will form. The impossibility of the methyl group to occupy the pocket at the end of the tunnel, due to the adoption of a different conformation or the acyl chain being shorter, maintaining the CoA fixation point, has consequences: a substrate below 18C could have a pitching movement within the tunnel. At the same time, the acyl chain could adopt different conformations. Both effects would contribute to changing the position of the C9-C10 bound within the tunnel. Spatial variations of the most effective position for the enzyme could justify a lower efficiency in the desaturation of fatty acids of less than 18C. Thus, our data show that Sea bass SCD 1b desaturates palmitic acid (C16: 0) with about 50% less efficiency than stearic acid (C18: 0).

Taken together, these finding suggest that the maximum size of the substrate is determined by the fact that the end of the tunnel is capped by seven amino acids, which define the site where the methyl group of the acyl chain should be located. Both, the tunnel volume and the possibility the acyl chain adopts less favorable conformations, could explain the ability of the enzyme to desaturate at n-7 position on 18C fatty acids and to transform fatty acids of less than 18C. In both cases, with less efficiency than for n-9 activity over 18C fatty acids. However, this low substrate specificity, which in principle could be considered a functional disadvantage, can be understood as a biological advantage: the enzyme is broad versatile, being able to desaturate substrates of different lengths and in different positions, to meet a broader need for mono-unsaturated fatty acids. That results in an enzyme that exhibits group specificity.

4.4. scd and Δ6 fad genes expression in European sea bass tissues

As in other species, *scd 1b* gene is widely but differently expressed in Sea bass tissues. Our results showed that the liver and adipose tissue are the tissues with the biggest transcription of *scd1b* gene. Brain, gonad and heart showed a smaller transcription, being the intestine the tissue that showed the lowest transcription level. In other species like mouse, rat or human and in mammals in general, the highest expression has been reported in liver and adipose tissue. In grass carp (*C. idella*) also was reported the highest expression in liver and in adipose tissue, followed of the brain (Chang et al., 2001) as well as in milkfish (*C. chanos*) (Hsieh et al., 2001), common carp (*C. carpio*) (Polley et al., 2003) and tilapia (*Oreochromis niloticus*) (Hsieh et al., 2003). The liver is the organ involved in lipid homeostasis, and the main function of the adipose tissue is the reserve of fatty acids that will be used when the organism needs to produce energy.

The proper maintenance of the plasma membrane fluidity in all physiological situations, also explains the high expression of this enzyme in the brain, with a particular unsaturated phospholipid composition in their membranes (24:1n-9, nervonic acid), allowing them to fulfil their important role (Mauvoisin and Mounier, 2011).

Furthermore, the profile of Δ6 FAD transcription in different tissues was evaluated. As previously shown González-Rovira et al. (2009), *Δ6 fad* gene was expressed in all tested tissues, being highest in brain, which is in concordance with previous results and the role of Δ6 FAD in the bioconversion pathway from eicosapentaenoic acid (EPA, 20:5n-3) to docosahexaenoic acid (DHA, 22:6n-3), (desaturation via of C24 HUFA intermediates or Sprecher pathway) (Sprecher, 2000). The high relative expression of Δ6 FAD and Elovl5 in the brain of several fish species has suggested an alternative role for these enzymes in marine fish, based on a requirement to maintain membrane DHA levels, particularly in neural tissues (Morais et al., 2011).

In all tested tissues, Δ6 FAD expression was smaller than the SCD 1b expression. The presence in both, SCD and Δ6 FAD mRNAs, of regulator elements of the expression above described, could explain the relatively high levels of SCD 1b mRNA and low levels of Δ6 FAD mRNA detected in all analyzed tissues. A big availability of SCD mRNA always, allows a fast response to promote a quick increment of monoenes. From a physiological point of view, the proper maintenance of the plasma membrane fluidity in all physiological situations explains the high expression of this

enzyme in all tissues. From a metabolic point of view, the high levels of SCD mRNA comparing to those of Δ6 FAD, clearly indicates that the SCD enzyme mainly drives the FAD activity. However, when the SCD/Δ6 FAD relative transcription ratio (RTR) is analyzed, could appreciate that it is different for each tissue, being the adipose tissue (474.43), the liver (148.01) and the heart (116.30) the tissues showing the biggest RTR values in the moment of the analysis. The high values of RTR suggest that in these tissues the SCD activity could be predominant and more outstanding and relevant in the desaturation process than Δ6 FAD activity. In contrast, gonad (24.41), brain (6.1) and intestine (3.54) RTR values suggest the biggest relative relevance of Δ6 FAD activity in these tissues. These results support the hypothesis that the presence of the Δ6 FAD activity in a marine teleost species is directed to assure enough quantity of 22:6n-3 in neural tissues (Tocher, 2010). However, which is the main role of Δ6 FAD in other tissues is still to be explained.

5. Conclusions

In this study, we have cloned, in silico and functionally characterized a new SCD 1b cDNA from European sea bass, an enzyme that is involved in the biosynthesis of MUFA. The protein appears highly conserved between different species and is localized in the ER. The *scd* gene is transcribed as two messengers of 3.5 and 1.4 kb. The level of transcription is higher in the liver followed by adipose tissue to a greater extent, followed by brain, gonad and heart, and to a lesser extent in the intestine, suggesting the greater relevance of SCD 1b in the desaturation of fatty acids in the liver and adipose tissue. In contrast, Δ6 FAD seems to play a more relevant role in fatty acid desaturation in the intestine brain and gonad. Finally, we have obtained a 3D structure of the enzyme by homology modelling, from which it is deduced that a new histidine residue, external to the His-motifs, and an Asn residue, both belonging to a new motif NX_3H like, could be involved in the coordination of a ferrous ion essential for enzymatic activity. The distance between the two ferrous ions from the active site, the lack of the sixth coordinating ligand of each Fe^{2+}, as well as the lack of carboxylates in the nearby environment suggest that the activation of molecular oxygen in SCD 1b could occur through a new mechanism. Although Sea bass SCD 1b has a greater preference for 18C substrates, it shows group specificity, being able to desaturate fatty acids of different lengths and at different positions, with different efficiency. The existence of the pocket at the end of the tunnel, where the methyl group could be fixed, and the possibility of movement and the adoption of different conformations of the acyl chain in the large tunnel, could explain and justify the preference for 18C substrates and the group specificity shown by the SCD 1b enzyme from Sea bass. Once again, the plasticity of biomolecules (both receptor and ligand) shows relevance of this characteristic to explain its basic properties and functioning and to understand the molecular bases of life. In a few words, for the Sea bass SCD 1b size does matter.

Declaration of interests

The authors declare that they have no known competing financial interests or personal relationships that could have appeared to influence the work reported in this paper.

Acknowledgments

We thank Dr. Charles E. Martin for DTY-11A strain supply. We thank Dr. Manuel Jiménez Tenorio and Antonio López Sierra, for their invaluable help in using Autodock software. AGR was supported by a contract from Junta de Andalucía, Spain. This work was founded in part by a Grant to C.P. (P06-AGR-02129) from Junta de Andalucía, by a grant to C.P. and AGR (20DPBBCP20) from Departamento de Biomedicina, Biotecnología y Salud Pública from University of Cádiz and the European Commission Grant DG XIV RAFOA Q5RS-2000-30058. Sequencing analyses were performed in the Servicio Central de Ciencia y Tecnología, Universidad de Cádiz, Spain.

Appendix A. Supplementary data

Supplementary data to this article can be found online at https://doi.org/10.1016/j.cbpb.2021.110698.

References

Abe, T., Sakuradani, E., Asano, T., Kanamaru, H., Shimizu, S., 2006. Functional characterization of Δ9 and ω9 desaturase genes in Mortierella alpina 1S-4 and its derivative mutants. Appl. Microbiol. Biotechnol. 70 (6), 711–719.

Aki, T., Shimada, Y., Inagaki, K., Higashimoto, H., Kawamoto, S., Shigeta, S., Ono, K., Suzuki, O., 1999. Molecular cloning and functional characterization of rat delta-6 fatty acid desaturase. Biochem. Biophys. Res. Commun. 255 (3), 575–579.

APROMAR, 2020. La acuicultura en España, p. 2020. http://www.apromar.es.

Bai, Y., McCoy, J.G., Levin, E.L., Sobrado, P., Rajashankar, K.R., Fox, B.G., Zhou, M., 2015. X-ray structure of a mammalian stearoyl-CoA desaturase. Nature 524 (7564), 252–256.

Benedito-Palos, L., Calduch-Giner, J.A., Ballester-Lozano, G.F., Pérez-Sánchez, J., 2013. Effect of ration size on fillet fatty acid composition, phospholipid allostasis and mRNA expression patterns of lipid regulatory genes in gilthead sea bream (*Sparus aurata*). Br. J. Nutr. 109 (7), 1175–1187.

Bernsel, A., Viklund, H., Hennerdal, A., Elofsson, A., 2009. TOPCONS: consensus prediction of membrane protein topology. Nucleic Acids Res. 37 (Web server issue), W465-8.

Buonocore, F., Libertini, A., Prugnoli, D., Mazzini, M., Scapigliati, G., 2006. Production and characterization of a continuous embryonic cell line from sea bass (*Dicentrarchus labrax* L.). Mar. Biotechnol. 8, 80–85.

Castro, L.F.C., Wilson, J.M., Gonçalves, O., Galante-Oliveira, S., Rocha, E., Cunha, I., 2011. The evolutionary history of the steroyl-CoA desaturase gene family in vertebrates. BMC Evol. Biol. 11, 132 https://doi.org/10.1186/1471-2148-11-132.

Chang, B.E., Hsieh, S.L., Kuo, C.M., 2001. Molecular cloning of full-length cDNA encoding delta-9 desaturase through PCR strategies and its genomic organization and expression in grass carp (*Ctenopharyngodon idella*). Mol. Reprod. Dev. 58 (3), 245–254.

Cho, H.P., Nakamura, M.T., Clarke, S.D., 1999a. Cloning, expression, and nutritional regulation of the mammalian Δ6 desaturase. J. Biol. Chem. 274 (1), 471–477.

Cho, H.P., Nakamura, M.T., Clarke, S.D., 1999b. Cloning, expression, and fatty acid regulation of the human Δ5 desaturase. J. Biol. Chem. 274 (52), 37335–37339.

Cossins, A.R., Bowler, K., 1987. Rate compensations and capacity adaptations. In: Temperature Biology of Animals. Springer, Netherlands, pp. 155–203.

Eigenheer, A.L., Young, S., Blomquist, G.J., Borgeson, C.E., Tillman, J.A., Tittiger, C., 2002. Isolation and characterization of *Musca domestica* delta-9 desaturase sequences. Insect Mol. Biol. 11 (6), 533–542.

Evans, H., De Tomaso, T., Quail, M., Rogers, J., Gracey, A., Cossins, A.R., Berenbrink, M., 2008. Ancient and modern duplication events and the evolution of stearoyl-CoA desaturases in teleost fishes, 35 (1), 18–29.

Felsenstein, J., 1985. Confidence limits on phylogenies: an approach using the bootstrap. Evolution. 39, 783–791.

Flowers, M.T., Ntambi, J.M., 2008. Role of stearoyl-coenzyme A desaturase in regulating lipid metabolism. Curr. Opin. Lipidol. 19 (3), 248–256.

Folch, J., Lees, M., Stanley, G.H.S., 1957. A simple method for the isolation and purification o total lipids from animal tissues. J. Biol. Chem. 226, 497–509.

González-Rovira, A., Mourente, G., Zheng, X., Tocher, D.R., Pendón, C., 2009. Molecular and functional characterization and expression analysis of a Δ6 fatty acyl desaturase cDNA of European Sea bass (*Dicentrarchus labrax* L.). Aquaculture 298 (1–2), 90–100.

Guillou, H., D'Andrea, S., Rioux, V., Barnouin, R., Dalaine, S., Pedrono, F., Legrand, P., 2004. Distinct roles of endoplasmic reticulum cytochrome b5 and fused cytochrome b5-like domain for rat Δ6-desaturase activity. J. Lipid Res. 45 (1), 32–40.

Hastings, N., Agaba, M., Tocher, D.R., Leaver, M.J., Dicks, J.R., Sargent, J.R., Teale, A.J., 2001. A vertebrate fatty acid desaturase with Δ5 and Δ6 activities. Proc. Natl. Acad. Sci. U. S. A. 98, 14304–14309.

Heinemann, F.S., Ozols, J., 2003. Stearoyl-CoA desaturase, a short-lived protein of endoplasmic reticulum with multiple control mechanisms. Prostaglandins Leukot. Essent. Fat. Acids 68 (2), 123–133.

Hsieh, S.L., Liao, W.L., Kuo, C.M., 2001. Molecular cloning and sequence analysis of stearoyl-CoA desaturase in milkfish, *Chanos chanos*. Comp. Biochem. Physiol. B: Biochem. Mol. Biol. 130 (4), 467–477.

Hsieh, S.L., Liu, R.W., Wu, C.H., Cheng, W.T., Kuo, C.M., 2003. cDNA nucleotide sequence coding for stearoyl-CoA desaturase and its expression in the zebrafish (*Danio rerio*) embryo. Mol. Reprod. Dev. 66 (4), 325–333.

Hsieh, S.L., Chang, H.T., Wu, C.H., Kuo, C.M., 2004. Cloning, tissue distribution and hormonal regulation of stearoyl-CoA desaturase in tilapia, *Oreochromis mossambicus*. Aquaculture. 230 (1–4), 527–546.

Jasniewski, A.J., Que Jr., L., 2018. Dioxygen activation by nonheme diiron enzymes: diverse dioxygen adducts, high-valent intermediates, and related model complexes. Chem. Rev. 118, 2554–2592. https://doi.org/10.1021/acs.chemrev.7b00457.

Kandasamy, P., Vemula, M., Oh, C.S., Chellappa, R., Martin, C.E., 2004. Regulation of unsaturated fatty acid biosynthesis in Saccharomyces: the endoplasmic reticulum membrane protein, Mga2p, a transcription activator of the OLE1 gene, regulates the

stability of the OLE1 mRNA through exosome-mediated mechanisms. J. Biol. Chem. 279 (35), 36586–36592.
Kelley, L.A., Mezulis, S., Yates, C.M., Wass, M.N., Sternberg, M.J.E., 2015. The Phyre2 web portal for protein modeling, prediction and analysis. Nat. Protoc. 10, 845–858.
Kenyon, J.R., Craig, I.W., 1999. Analysis of the 5′ regulatory region of the human Norrie's disease gene: evidence that a non-translated CT dinucleotide repeat in exon one has a role in controlling expression. Gene 227, 181–188.
Kerppola, T.K., Curran, T., 1994. A conserved region adjacent to the basic domain is required for recognition of an extended DNA binding site by Maf/Nrl family proteins. Oncogene 9 (11), 3149–3158.
Krieger, E., Joo, K., Lee, J., Lee, J., Raman, S., Thompson, J., Tyka, M., Baker, D., Karplus, K., 2009. Improving physical realism, stereochemistry, and side-chain accuracy in homology modeling: four approaches that performed well in CASP8. Proteins 77 (Suppl. 9), 114–122.
Leonard, A.E., Bobik, E.G., Dorado, J., Kroeger, P.E., Chuang, L.T., Thurmond, J.M., Parker- Barnes, J.M., Das, T., Huang, Y.S., Mukerji, P., 2000. Cloning of a human cDNA encoding a novel enzyme involved in the elongation of long-chain polyunsaturated fatty acids. Biochem. J. 350, 765–770.
Li, Q., Lau, A., Morris, T.J., Guo, L., Fordyce, C.B., Stanley, E.F., 2004. A syntaxin 1, Galphao, and N-Type calcium channel complex at a presynaptic nerve terminal: analysis by quantitative immunocolocalization. J. Neurosci. 24, 4070–4081.
Manders, E., Stap, J., Brakenhoff, G., van Driel, R., Aten, J., 1992. Dynamics of three-dimensional replication patterns during the S-phase, analysed by double labelling of DNA and confocal microscopy. J. Cell Sci. 103, 857–862.
Marquardt, A., Stöhr, H., White, K., Weber, B.H., 2000. cDNA cloning, genomic structure, and chromosomal localization of three members of the human fatty acid desaturase family. Genomics 66 (2), 175–183.
Mauvoisin, D., Mounier, C., 2011. Hormonal and nutritional regulation of SCD1 gene expression. Biochimie 93 (1), 78–86.
Meesapyodsuk, D., Qiu, X., 2014. Structure determinants for the substrate specificity of acyl-CoA Δ9 desaturases from a marine copepod. ACS Chem. Biol. 9 (4), 922–934.
Mihara, K., 1990. Structure and regulation of rat liver microsomal stearoyl-CoA desaturase gene. J. Biochem. 108 (6), 1022–1029.
Mitchell, A.G., Martin, C.E., 1995. A novel cytochrome b- like domain is linked to the carboxyl terminus of the *Saccharomyces cerevisiae* Δ-9 fatty acid desaturase. J. Biol. Chem. 270 (50), 29766–29772.
Miyazaki, M., Bruggink, S.M., Ntambi, J.M., 2006. Identification of mouse palmitoyl-coenzyme a Δ9-desaturase. J. Lipid Res. 47, 700–704. https://doi.org/10.1194/jlr.C500025-JLR200.
Monroig, O., de Llanos, R., Varó, I., Hontoria, F., Tocher, D.R., Puig, S., Navarro, J.C., 2017. Biosynthesis of polyunsaturated fatty acids in octopus vulgaris: molecular cloning and functional characterisation of a stearoyl-CoA desaturase and an elongation of very long-chain fatty acid 4 protein. Mar. Drugs 15, 82. https://doi.org/10.3390/md15030082.
Morais, S., Mourente, G., Ortega, A., Tocher, J.A., Tocher, D.R., 2011. Expression of fatty acyl desaturase and elongase genes, and evolution of DHA:EPA ratio during development of unfed larvae of Atlantic bluefin tuna (*Thunnus thynnus* L.). Aquaculture 313, 129–139.
Muñoz, I., Sepulcre, M.P., Meseguer, J., Mulero, V., 2014. Toll- like receptor 22 of gilthead sea bream, *Sparus aurata*: molecular cloning, expression profiles and post-transcriptional regulation. Dev. Comp. Immunol. 44 (1), 173–179.
Nakamura, M.T., Nara, T.Y., 2004. Structure, function, and dietary regulation of Δ6, Δ5, and Δ9 desaturases. (2004). Annu. Rev. Nutr. 24, 345–376.
Napier, J.A., Hey, S.J., Lacey, D.J., Shewry, P.R., 1998. Identification of a *Caenorhabditis elegans* Δ6-fatty-acid-desaturase by heterologous expression in *Saccharomyces cerevisiae*. Biochem. J. 330, 611–614.
Nei, M., Kumar, S., 2000. Molecular Evolution and Phylogenetic. Oxford University Press, New York.
Ntambi, J.M., 1999. Regulation of stearoyl-CoA desaturase by polyunsaturated fatty acids and cholesterol. J. Lipid Res. 40 (9), 1549–1558.
Oku, H., Umino, T., 2008. Molecular characterization of peroxisome proliferator-activated receptors (PPARs) and their gene expression in the differentiating adipocytes of red sea bream *Pagrus major*. Comp. Biochem. Physiol. B: Biochem. Mol. Biol. 151 (3), 268–277.
Paton, C.M., Ntambi, J.M., 2009. Biochemical and physiological function of steroyl-CoA desaturase. Am. J. Physiol. Endocrinol. Metab. 297 (1), E28–E37.
Pendón, C., Martinez-Barberá, J.P., Perez-Sanchez, J., Rodríguez, R.B., Grenett, H., Valdivia, M.M., 1994. Cloning of the sole (*Solea senegalensis*) growth hormone-encoding cDNA. Gene. 145 (2), 237–240.
Pettersen, E.F., Goddard, T.D., Huang, C.C., Couch, G.S., Greenblatt, D.M., Meng, E.C., Ferrin, T.E., 2004. UCSF Chimera—a visualization system for exploratory research and analysis. J. Comput. Chem. 25 (13), 1605–1612.
Polley, S.D., Tiku, P.E., Trueman, R.T., Caddick, M.X., Morozov, I.Y., Cossins, A.R., 2003. Differential expression of cold- and diet- specific genes encoding two carp liver Δ9-acyl-CoA desaturase isoforms. Am. J. Phys. Regul. Integr. Comp. Phys. 284, R41–R50.
Saitou, N., Nei, M., 1987. The neighbor-joining method: a new method for reconstructing phylogenetic trees. Mol. Biol. Evol. 4, 406–425.
Savan, R., 2014. Post-transcriptional regulation of interferons and their signaling pathways. J. Interf. Cytokine Res. 34 (5), 318–329.
Shanklin, J., Whittle, E., Fox, B.G., 1994. Eight histidine residues are catalytically essential in a membrane-associated iron enzyme, stearoyl-CoA desaturase, and are conserved in alkane hydroxylase and xylene monooxygenase. Biochemistry. 33 (43), 12787–12794.
Shen, J., Wu, G., Tsai, A., Zhou, M., 2020. Structure and mechanism of a unique di-iron center in mammalian stearoyl-CoA desaturase. J. Mol. Biol. 432, 5152–5161.
Sprecher, H., 2000. Metabolism of highly unsaturated n-3 and n- 6 fatty acids. Biochim. Biophys. Acta 1486, 219–231.
Stukey, J.E., McDonough, V.M., Martin, C.E., 1990. The OLE1 gene of *Saccharomyces cerevisiae* encodes the delta 9 fatty acid desaturase and can be functionally replaced by the rat stearoyl-CoA desaturase gene. J. Biol. Chem. 265 (33), 20144–20149.
Tamura, K., Stecher, G., Peterson, D., Filipski, A., Kumar, S., 2013. MEGA6: molecular evolutionary genetics analysis version 6.0. Mol. Biol. Evol. 30, 2725–2729.
Tian, W., Chen, C., Lei, X., Zhao, J., Liang, J., 2018. CASTp 3.0: computed atlas of surface topography of proteins. Nucleic Acids Res. 46, W363–W367. https://doi.org/10.1093/nar/gky473. Issue W1, 2.
Tiku, P.E., Gracey, A.Y., Macartney, A.I., Beynon, R.J., Cossins, A.R., 1996. Cold-induced expression of Δ9-desaturase in carp by transcriptional and posttranslational mechanisms. Science 271 (5250), 815–818.
Tocher, D.R., 2010. Fatty acid requirements in ontogeny of marine and freshwater fish. Aquac. Res. 41, 717–732.
Tocher, D.R., Leaver, M.J., Hodgson, P.A., 1998. Recent advances in the biochemistry and molecular biology of fatty acyl desaturases. Prog. Lipid Res. 37 (2–3), 73–117.
Tusnády, G.E., Simon, I., 1998. Principles "governing amino acid composition of integral membrane proteins: applications to topology prediction". J. Mol. Biol. 283, 489–506.
Tusnády, G.E., Simon, I., 2001. The new features of HMMTOP 2.0 version is described in the HMMTOP transmembrane topology prediction server. Bioinformatics 17, 849–850.
Vasudevan, S., Peltz, S.W., 2001. Regulated ARE-mediated mRNA decay in *Saccharomyces cerevisiae*. Mol. Cell 7 (6), 1191–1200.
Vemula, M., Kandasamy, P., Oh, C.S., Chellappa, R., González, C.I., Martin, C.E., 2003. Maintenance and regulation of mRNA stability of the *Saccharomyces cerevisiae* OLE1 gene requires multiple elements within the transcript that act through translation-independent mechanisms. J. Biol. Chem. 278 (46), 45269–45279.
Veyrune, J.L., Hesketh, J., Blanchard, J.M., 1997. 3′untranslated regions of c-myc and c-fos mRNAs: multifunctional elements regulating mRNA translation, degradation and subcellular localization. In: Jeanteur, P. (Ed.), Cytoplasmic Fate of Messenger RNA, 18. Springer, Berlin Heidelberg, pp. 35–63.
Wang, J., Yu, L., Schmidt, R.E., Su, C., Huang, X., Gould, K., Cao, G., 2005. Characterization of HSCD5, a novel human stearoyl- CoA desaturase unique to primates. Biochem. Biophys. Res. Commun. 332 (3), 735–742.
Wang, H., Klein, M.G., Zou, H., Lane, W., Snell, G., Levin, I., Li, K., Sang, B.C., 2015. Crystal structure of human stearoyl-coenzymeA in complex with substrate. Nat. Struct. Mol. Biol. 22, 581–585. https://doi.org/10.1038/nsmb.3049.
Watts, J.L., Browse, J., 1999. Isolation and characterization of a Delta 5-fatty acid desaturase from *Caenorhabditis elegans*. Arch. Biochem. Biophys. 362 (1), 175–182.
Weng, C.M., Miyazaki, M., Chu, K., Ntambi, J.M., 2006. Membrane topology of mouse stearoyl-CoA desaturase. J. Biol. Chem. 281 (2), 1251–1260.
Wodtke, E., Cossins, A.R., 1991. Rapid cold-induced changes of membrane order and Δ9-desaturase activity in endoplasmic reticulum of carp liver: a time-course study of thermal acclimation. Biochim. Biophys. Acta Biomembr. 1064 (2), 343–350.
Wu, X., Zou, X., Chang, Q., Zhang, Y., Li, Y., Zhang, L., Huang, J., Lianng, B., 2013. The evolutionary pattern and the regulation of stearoyl-CoA desaturase genes. Biomed. Res. Int. 2013. Article ID 856521.
Yadav, M.P., Igartuburu, J.M., Yan, Y., Nothnagel, E.A., 2007. Chemical investigation of the structural basis of the emulsifying activity of gum arabic. Food Hydrocoll. 21 (2), 297–308.
Yuan, Z., Mattick, J.S., Teasdale, R.D., 2004. SVMtm: support vector machines to predict transmembrane segments. J. Comput. Chem. 25 (5), 632–636.
Zar, J.H., 1984. Biostatistical Analysis, 2nd ed. Prentice-Hall, Englewood Cliffs, NJ.
Zhang, L., Ge, L., Parimoo, S., Stenn, K., Prouty, S.M., 1999. Human stearoyl-CoA desaturase: alternative transcripts generated from a single gene by usage of tandem polyadenylation sites. Biochem. J. 340 (1), 255–264.
Zhang, R., Zhu, L., Zhang, Y., Shao, D., Wang, L., Gong, D., 2013. cDNA cloning and the response to overfeeding in the expression of stearoyl-CoA desaturase 1 gene in *Landes goose*. Gene. 512 (2), 464–469.